ACKNOWLEDGEMENT

This research was performed within the Faculty of Civil Engineering and Management, section Water Engineering & Management of the University of Twente. I am grateful I was given the opportunity to be part of this research group when conducting my research and could because of that enjoy the encouraging words of faculty and room members when drinking coffee.

But within this faculty special thanks goes out to my personal mentor, dr. ir. Pieter C. Roos, whom always believed in my capabilities even if I sometimes didn't. You really made me enjoy sandbanks, even though it are just (almost imperturbable) sand accumulations!

Secondly I wanted to thank my supervisor Prof. dr. Suzanne J. M. H. Hulscher whom always came with challenging questions and advise. And even if I sometimes wished she rather didn't, they made this research as well grounded and complete as it is.

And finally I wanted to thank my external committee member Dr. Ruud T.E. Schüttenhelm, whom was able to push me to criticize all literature as well as the origination of sandbanks in general.

Thank you all for making my final research into what it is, into what lies before you and into something that I am actually proud of.

ABSTRACT

The development of sandbanks as presently captured in morphodynamical models is assumed to occur under a constant waterdepth over time. This assumption needs to be reconsidered as it takes centuries to millennia for a sandbank to evolve towards equilibrium and during that same period the process of sea level rise may significantly change the average waterdepth. Therefore the possible influence of sea level rise on the sandbank morphodynamics is investigated within this project.

As this project is a first exploration of the possible connection between sea level rise and sandbank development this research is limited to the linear regime, which represent the initial stage of sandbank formation, to get a first impression. Hence the linear sandbank morphodynamical model as defined by Hulscher et al. [1993] is used to investigate the influence of changes in the waterdepth on the formation of sandbanks. Besides an increase of the waterdepth the process of sea level rise also captures the accompanying decrease in the flow velocity. Furthermore changes in the drag coefficient, the slope parameter and the latitude are taken into consideration to determine their additional influence on the development of sandbanks being subjected to sea level rise.

The influence of changes in the waterdepth is made visible by means of the four sandbank characteristics which can be retrieved from the linear model: growth rate, wavelength, angle of orientation and the migration speed. As this linear model represents only the initial development of sandbanks, the characteristics represent the preferred shape of the sandbank. The values found for each sandbank characteristic regarding changes in the waterdepth and the flow velocity are presented in graphs to clarify the changes in its development over time. Additionally the influences of changes in the drag coefficient, the slope parameter and the latitude on these developments are given.

Based upon this research it can be concluded that the angle of orientation is the least sensitive and the wavelength the most sensitive to a change in the waterdepth. The value of both characteristics increases due to an increasing waterdepth, which is amplified by changes in the drag coefficient for the wavelength and slope parameter for the angle of orientation. At the same time the growth rate and the migration speed decrease with increasing waterdepth of which the rate strongly depends on the change in flow velocity.

The final comparison of the development of the wavelength against increasing waterdepth as estimated by the model with the Dutch Banks, Flemish Banks and Zeeland Banks, with inclusion of Holocene deposits, show a good agreement.

INDEX

1 INTRODUCTION ..... - 6 -
2 BACKGROUND ON SANDBANKS ..... - 7 -
2.1 CLASSIFICATION ..... - 7 -
2.2 SANDBANKS IN THE NORTH SEA ..... - 8 -
2.3 SANDBANK MORPHODYNAMICS ..... - 9 -
2.3.1 THE INITIAL STAGE OF FORMATION ..... - 10 -
2.3.2 THE EVOLUTION TOWARDS EQUILIBRIUM ..... - 12 -
2.3.3 A DIFFERENT APPROACH ..... - 14 -
2.3.4 APPLICATIONS ..... - 15 -
2.3.5 DISCUSSION ..... - 15 -
3 SEA LEVEL RISE ..... - 16 -
3.1 GLOBAL SEA LEVEL RISE ..... - 16 -
3.2 THE SOUTHERN NORTH SEA ..... - 18 -
3.2.1 SEA LEVEL RISE DURING THE PAST 9,000 YEARS ..... - 19 -
4 INFLUENCE OF SEA LEVEL RISE ON SANDBANKS ..... - 23 -
5 MATHEMATICAL DESCRIPTION OF A LINEAR MODEL ..... - 24 -
5.1 MODEL FORMULATION ..... - 24 -
5.1.1 LINEAR STABILITY: THE BASIC STATE ..... - 26 -
6 METHODOLOGY FOR CONDUCTING A SENSITIVITY ANALYSIS ..... - 29 -
6.1 RESEARCH OBJECTIVE ..... - 30 -
6.2 PARAMETER SPECIFICATION ..... - 30 -
6.3 VARIATION IN PARAMETER VALUES ..... - 32 -
6.4 ANALYSIS PROCEDURE ..... - 33 -
7 RESULTS ..... - 34 -
7.1 GROWTH RATE ..... - 34 -
7.2 ANGLE OF ORIENTATION ..... - 35 -
7.3 WAVELENGTH ..... - 36 -
7.4 MIGRATION SPEED ..... - 37 -
8 DISCUSSION ..... - 38 -
8.1 METHOD ..... - 38 -
8.2 MODEL ..... - 42 -
9 A COMPARISON WITH REALITY ..... - 43 -
9.1 PRESENT SITUATION ..... - 43 -
9.2 DEVELOPMENT OVER THE PAST 9,000 YEARS ..... - 45 -
10 CONCLUSIONS AND RECOMMENDATIONS ..... - 48 -
10.1 CONCLUSIONS ..... - 48 -
10.2 RECOMMENDATIONS ..... - 49 -
11 REFERENCES ..... - 50 -
APPENDIX A: THE GROWTH RATE ..... - 54 -
APPENDIX B: ANGLE OF ORIENTATION ..... - 55 -
APPENDIX C: THE WAVELENGTH ..... - 56 -
APPENDIX D: THE MIGRATION SPEED ..... - 57 -
APPENDIX E: COMPARISON WITH REALITY ..... - 58 -

TABLE OF FIGURES

Figure 1: Flemish Banks Group ..... - 7 -
Figure 2: Indian River Estuary ..... - 7 -
Figure 3: Cape Romain, South Carolina ..... - 8 -
Figure 4: (1) Open shelf ridge (2A) Estuary mouth ridge (2Bi) Estuary ebb tidal delta (2Bii) Estuary shoreface connected ridge (3A) Banner Banks (3B) Alternating Ridges ..... - 8 -
Figure 5: Morphodynamics of sandbanks ..... - 9 -
Figure 6: Development of infinite perturbation ..... - 10 -
Figure 7: Wavelength and orientation ..... - 11 -
Figure 8: Wave vector against mean flow ..... - 12 -
Figure 9: Formation of sandbanks out of sand waves ..... - 14 -
Figure 10: Tide gauge ..... - 16 -
Figure 11: Geological Time table ..... - 18 -
Figure 12: Southern Bight North Sea ..... - 19 -
Figure 13: Relative sea level rises ..... - 20 -
Figure 14: North Sea conditions 9,000 years Bp: *Left*: tide induced change in local mean sea level, *Middle:* current ellipses, *Right:* M_2-tide co-tidal charts ..... - 20 -
Figure 15: North Sea conditions 8,500 years Bp: *Left*: tide induced change in local mean sea level, *Middle:* current ellipses, *Right:* M_2-tide co-tidal charts ..... - 21 -
Figure 16: North Sea conditions 7,000 years Bp: *Left*: tide induced change in local mean sea level, *Middle:* current ellipses, *Right:* M_2-tide co-tidal charts ..... - 21 -
Figure 17: Present North Sea conditions: *Left*: tide induced change in local mean sea level, *Middle:* current ellipses, *Right:* M_2-tide co-tidal charts. ..... - 22 -
Figure 18: Sketch of offshore location ..... - 24 -
Figure 19: Waterdepths in the North Sea ..... - 32 -
Figure 20: Flow velocities in the North Sea ..... - 32 -
Figure 21: Growth rate against waterdepth; *Upper*: constant flow velocity *Lower*: constant water flux ..... - 34 -
Figure 22: Counter clockwise orientation against waterdepth; *Upper*: constant flow velocity, *Lower*: constant water flux ..... - 35 -
Figure 23: Wavelength against waterdepth for both approaches ..... - 36 -
Figure 24: Migration speed against waterdepth; *Upper*: constant flow velocity *Lower*: constant water flux ..... - 37 -
Figure 25: Example of the range of a graph ..... - 40 -
Figure 26: The three sandbank groups; *Upper:* Dutch Banks, *Middle:* Zeeland Banks, *Lower:* Flemish Banks ..... - 43 -
Figure 27: Growth Rate against increasing waterdepth for different values of the drag coefficient; *Left*: Constant Flow Velocity, *Right*: Constant Water Flux. ..... - 54 -
Figure 28: Growth Rate against increasing waterdepth for different values of the slope factor; *Left*: Constant Flow Velocity; *Right*: Constant Water Flux. ..... - 54 -
Figure 29: Growth Rate against increasing waterdepth for different values of the latitude; *Left*: Constant Flow Velocity; *Right*: Constant Water Flux. ..... - 54 -

Figure 30: Counter clockwise angle of orientation against increasing waterdepth for the drag coefficient; *Left*: Constant Flow Velocity; *Right*: Constant Water Flux .... - 55 -
Figure 31: Counter clockwise angle of orientation against increasing waterdepth for the slope factor; *Left*: Constant Flow Velocity; *Right*: Constant Water Flux ..... - 55 -
Figure 32: Counter clockwise angle of orientation against increasing waterdepth for the latitude; *Left*: Constant Flow Velocity; *Right*: Constant Water Flux..... - 55 -
Figure 33: Wavelength against increasing waterdepth for the drag coefficient; *Left*: Constant Flow Velocity; *Right*: Constant Water Flux ..... - 56 -
Figure 34: Wavelength against increasing waterdepth for the slope parameter: *Left*: Constant Flow Velocity; *Right*: Constant Water Flux ..... - 56 -
Figure 35: Wavelength against increasing waterdepth for the latitude; *Left*: Constant Flow Velocity; *Right*: Constant Water Flux ..... - 56 -
Figure 36: Migration speed against increasing waterdepth for the drag coefficient; *Left*: Constant Flow Velocity; *Right*: Constant Water Flux ..... - 57 -
Figure 37: Migration speed against increasing waterdepth for the slope factor: *Left*: Constant Flow Velocity; *Right*: Constant Water Flux ..... - 57 -
Figure 38: Migration speed against increasing waterdepth for the latitude; *Left*: Constant Flow Velocity; *Right*: Constant Water Flux ..... - 57 -
Figure 39: The average flow velocity in the North Sea..... - 58 -
Figure 40: Holocene sediment deposits in the Southern North Sea..... - 58 -

TABLE OF TABLES

Table 1: Sea level change past 8,000 years ..... - 23 -
Table 2: Sensitivity of sandbank characteristics to changes in the Constant Water Flux (C.W.F) or Constant Flow Velocity (C.F.V.) ..... - 39 -
Table 3: Influences of parameters to the basic lines of the Constant Flow Velocity (C.F.V) and Constant Water Flux (C.W.F) approach per sandbank characteristic expressed in quadratic means and percentage. ..... - 40 -
Table 4 Sandbank characteristics, average waterdepth and flow velocity. The flow velocity is estimated from figure X, Appendix E, and the average waterdepth for the Zeeland Banks is estimated from figure 19..... - 44 -
Table 5: Model results based upon the average waterdepth and flow velocity. ..... - 44 -
Table 6: Wavelength 9,000 – 8,500 years BP for different sandbanks, different waterdepths and both assumptions: Constant Flow Velocity (C.F.V.) and Constant Water Flux (C.W.F.) ..... - 46 -
Table 7: Wavelength 8,500 – 7,000 years BP for different sandbanks, different waterdepths and both assumptions: Constant Flow Velocity (C.F.V.) and Constant Water Flux (C.W.F.) ..... - 46 -
Table 8:Wavelength 7,000 – 0 years BP for different sandbanks, different waterdepths and both assumptions: Constant Flow Velocity (C.F.V.) and Constant Water Flux (C.W.F.)..... - 47 -

1 INTRODUCTION

This report deals with the influence of sea level rise on sandbank morphodynamics. The idea for this research originated from earlier research on capturing the origin and development of sandbanks within morphodynamical models. So far these models adopted a constant waterdepth, but as it takes centuries to millennia for a sandbank to develop towards a mature stage it is not likely for the waterdepth to stay constant over that period. Therefore the main objective of this research is:

What is the influence of sea level rise on sandbank morphodynamics?

This report starts with a background on sandbank morphodynamics in chapter 2. This involves different types of sandbanks but will focus on the case of tidal sandbanks. The reason for this is that the morphodynamics of tidal sandbanks is less complex compared to that of other features. Furthermore a lot of information on tidal sandbanks is available through earlier research, especially for the Southern Bight of the North Sea.

Chapter 3 covers the development of the sea level rise in the Southern Bight of the North Sea, preceded by a general introduction on the processes of sea level rise.

The typical time scales on which sandbanks develop and the sea level changes corresponds as explained in more detail in chapter 4. These first four chapters deal with the physical processes of sandbank morphodynamics, sea level rise and their possible connection. The model which is used to determine what influence sea level rise has on sandbank morphodynamics quantitatively, is presented in chapter 5.

To investigate the influence of sea level rise on sandbank morphodynamics by means of a model is called a sensitivity analysis, of which the methodology is explained in chapter 6. The modelled results are placed against their physical background in chapter 7. The restraints of the methodology as well as those of the used model by means of a robustness analysis are discussed in chapter 8.

Chapter 9 handles a comparison and discussion of the found changes in development of the wavelength due to an increasing waterdepth with the present conditions of the Dutch Banks, Zeeland Banks and Flemish Banks.

The overall conclusions which can be drawn from this research are given in chapter 10 together with some recommendations on possible further research to enhance the knowledge on sandbank formation.

2 BACKGROUND ON SANDBANKS

2.1 CLASSIFICATION

The sea bottom accommodates various features of different magnitude. On places with abundant sand and currents strong enough to move sediment, sandbanks and elongated sand ridges can develop. Distinction can be made between actively maintained sandbanks and those that have turned moribund, to be explained further on. The further division into tidal sandbanks, estuary mouth banks or headland banks is based on their morphology, hydrodynamics, geological origin or development. A more detailed discussion of this classification is given below [Dyer & Huntley, 1999].

TIDAL SANDBANKS

Tidal sandbanks, also known as open shelf ridges, appear in groups at places where the tidal current exceeds a speed of 0.5 ms^{-1} and enough sand is available. They are up to 80km long, average 13km wide and are up to tens of metres in height [Off, 1963]. Tidal sandbanks are often asymmetrical and it is thought that they gradually move in the direction of the steeper side. Dependent on the direction of the Coriolis force (clockwise in Southern Hemisphere, anticlockwise in the Northern) their oblique orientation to the tidal current can increase to 40°. They are often relatively broad and flat at one end and narrower and pointed at the other. They can originate from an excess of sand supply, be the equilibrium result of a sediment path or the remains of larger deposits [Caston, 1981]. Generally they are located on top of a platform of less mobile sediment or rock.

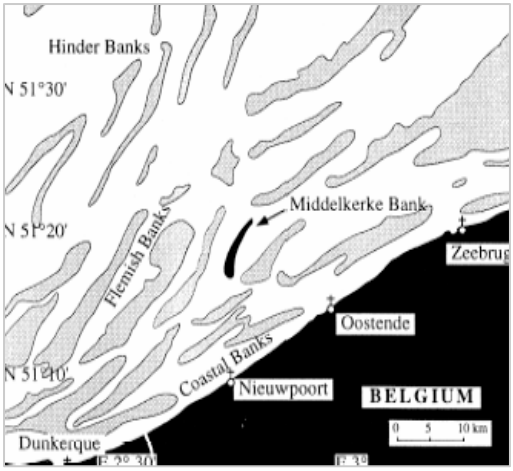

Figure 1: Flemish Banks Group [Dyer & Huntley, 1999]

ESTUARY MOUTH

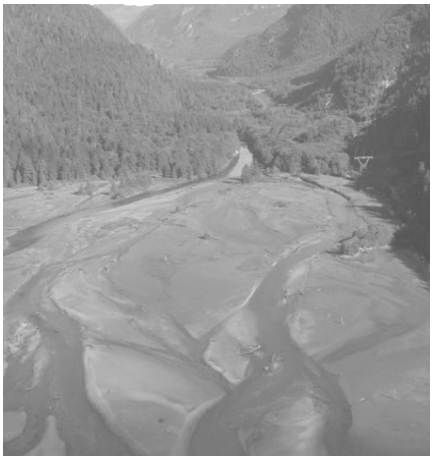

Estuary mouth sandbanks appear in two types: ridges and tidal deltas. The former are smaller than 10km and appear in the mouth of macro tidal deltas [Harris, 1988]. The latter, formed by meso or micro tidal deltas, are usually larger than 10km and can be further divided into shoreface connected ridges and ebb tidal deltas. The process behind their formation is the interaction between strong flood currents which are dominant in the channels and the weaker ebb currents dominating the shallower parts. For the ridges the net sediment transport is into the mouth resulting in a bed elevation there, whereas the deltas are formed by deposition of the seaward transported sediment.

Figure 2: Indian River Estuary [www.deepcovekayak.com]

HEADLAND BANKS

There are two types of headland banks: banner banks and alternating ridges. Both are formed due to changes in the alongshore sand transport rate. Banner banks are formed behind erosion resistant headlands or places where the sea bottom has a steep slope towards deeper water [Swift, 1975]. They are often pear-shaped (the higher part pointed seawards) and separated of the main land by a deep narrow channel. Alternating ridges are land parts which are detached from the main land due to a retreating shoreline caused by erosion or sea level rise.

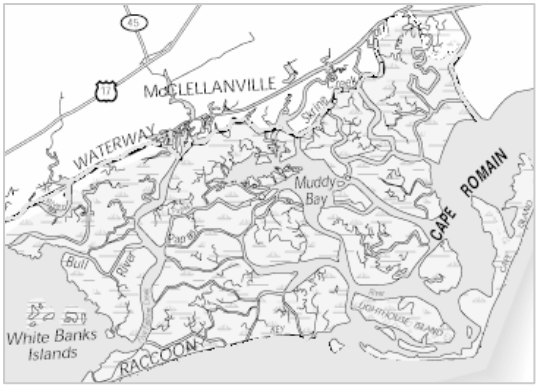

Figure 3: Cape Romain, South Carolina [www.caperomain.fws.gov]

MORIBUND RIDGES

The so-called moribund ridges are extinct features of all types as described above. They are located at places where the present peak currents are no longer capable of moving the sand [Belderson et al, 1986]. They can be distinguished from the actively maintained banks as their surrounding floor consists of fine sand or mud instead of clean medium sand to gravel. Furthermore, they have no large sand waves on their flanks, and have more round-crested cross-sections usually with a slope of about 1°. Sand waves and sandbanks are often confused as they both appear at the same places. Nevertheless their physical appearance is different: sand waves are smaller than sandbanks. Sand waves have a wavelength between 100-800m and height up to 5m, their crests are more or less parallel and elongated and orientated perpendicular or anastomosing to the flow direction [Terwindt, 1971].

2.2 SANDBANKS IN THE NORTH SEA

The Southern North Sea is an ideal study area as all types of the ridges introduced above are present; still developing or turned moribund. The dominating type in the North Sea is the tidal sandbank. The tidal sandbanks are chosen to form the subject of this research as their morphodynamics is less complex compared to that of other features, due to little changes in the restraining conditions over the sandbanks.

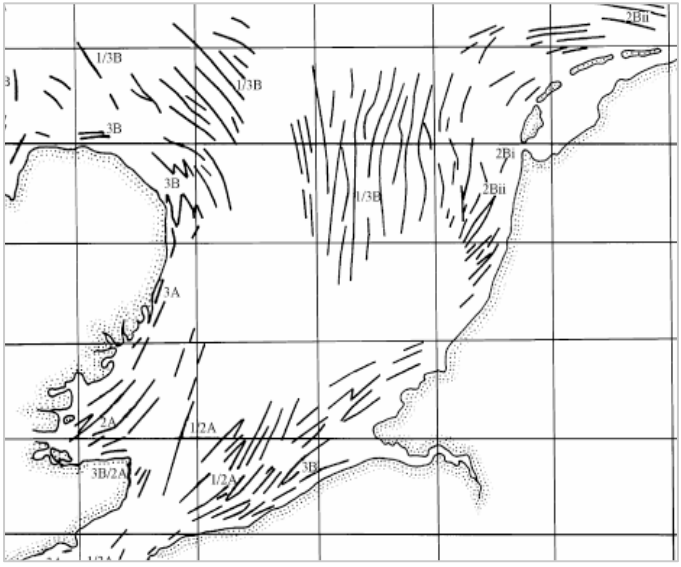

Figure 4: (1) Open shelf ridge (2A) Estuary mouth ridge (2Bi) Estuary ebb tidal delta (2Bii) Estuary shoreface connected ridge (3A) Banner Banks (3B) Alternating Ridges [Dyer & Huntley, 1999]

2.3 SANDBANK MORPHODYNAMICS

Morphodynamics is the combination of the words dynamics and morphology that describes the hydrodynamically driven system of interaction between the sea bed and the bed-load or suspended sediment transport that leads to the origination of sandbanks. To be able to describe the morphodynamics of tidal sandbanks briefly, the driving hydrodynamical processes and the sediment motion are explained below.

HYDRODYNAMICS

Tidal sandbanks are generated by interactions within the horizontal tidal system: the by the Coriolis force cum-sole deflected back and forth movement of the tidal current which enforces the water particles to follow a more-ore less elliptical path. In shallow seas it is usual for the tidal ellipses to be asymmetrical as the peak ebb and flow tidal currents tend to be unequal [Brown et al, 1999]. This originates partly from the interaction between tidal constituents of different periods and partly are tidal currents modified by coastline alignment, topography and local water conditions, which results in residual currents (long term net movements of water in fairly well defined directions). The tidal current is furthermore subject to vertical current shear enforced by friction with the sea bed i.e. change in current velocity with height above the bed.

SEDIMENT TRANSPORT

Sediment transport occurs if the flow velocity is of such speed that it enforces a stress on the bottom that is strong enough to set particles in motion. This minimal amount of stress needed to overcome the gravitational and adherent processes on the bottom is called the shear-stress threshold and depends not only on the flow velocity but also on the characteristics of the particles. In sediment transport, distinction is made between bed-load sediment transport (representing particles that stay in contact with the bed) and suspended sediment transport [Brown et al, 1999]. Besides the flow velocity and particle characteristics, the slope of the sea-bottom is also of influence on the amount of transport as particles are easier transported downhill enforced by gravity [Huthnance, 1982].

MORPHODYNAMICS

The morphodynamics of tidal sandbanks is the interaction between the horizontal movement of the tide and the sea bed. As explained under hydrodynamics the tidal flow currents in shallow seas are most often not symmetrical, resulting in deviations in the flow velocity. Additional this leads to changes in the sediment transport. This interaction is presented by the most inner box of figure 5. If the current is slowed down by an uneven sea bottom, resulting in sediment deposits after the irregularities, bed evolution can occur.

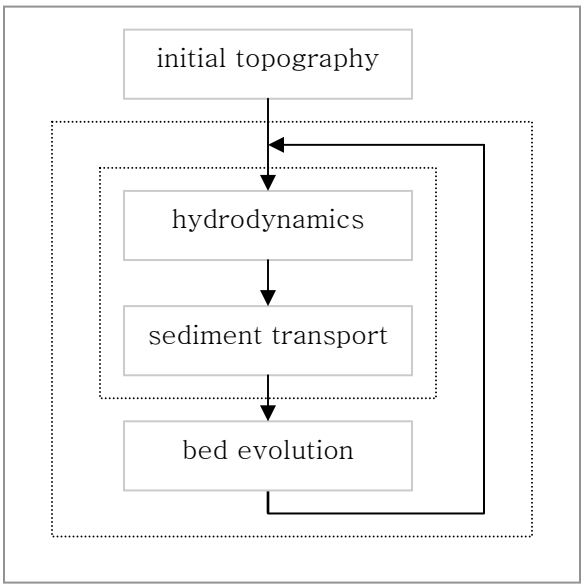

Figure 5: Morphodynamics of sandbanks [Roos and Hulscher, 2003]

Under which circumstances this evolution leads to sandbank formation, shall be explained in more detail in the next paragraph. The bed evolution will affect the flow as it changes the bathymetry which closes the circle in which sandbanks are formed. Earlier research pointed out that the initial development of sandbanks can be described through linear processes [Huthnance, 1982]. Once the sandbank becomes larger and evolves to equilibrium, these processes are no longer behaving linearly and it is necessary to formulate a non-linear model to capture their morphodynamics. In this chapter the literature on both stages of sandbank formation, initial and towards equilibrium, are described. Although using a linear model to describe the initial stage of sandbank formation is commonly adopted, the non-linear model as developed by Komarova and Newell [2000] is presented as well. This chapter also contains some practical applications of the models and ends with a discussion of the literature.

2.3.1 THE INITIAL STAGE OF FORMATION

Huthnance [1982] was the first to describe sandbanks as instability of the morphological system, as presented in figure 5. He described the motion of fluid by the shallow water equations, which are the depth averaged Navier-Stokes equations. Besides the adoption of a depth averaged flow, he assumed a uniform waterdepth and a sediment motion with a faster than linear dependence with the current and a downhill preference. If we consider a flat bottom the fluid motion during a tidal cycle is directed opposite to the flow direction during the other half, as is the sediment transport. In case of a symmetrical tide the flow over this bed is spatially uniform, resulting in zero tidal averaged sediment transport and bed evolution stays out. But the flow will be influenced by irregularities of the sea bottom. One irregularity is called a perturbation and if some perturbations are placed upon the sea bottom with a constant spacing and a length longer than the area under consideration (consider them infinite) in such way that the flow crosses them under an angle, the following developments occur:

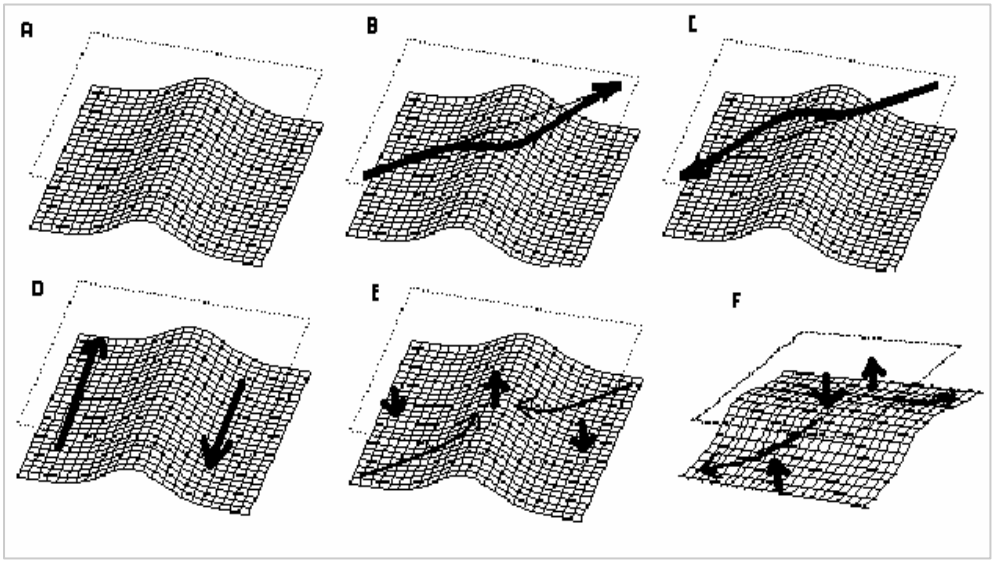

Figure 6: Development of infinite perturbation
A: infinite perturbation; **B/C**: bend of tidal flow during half a tidal period; **D:** tidal flow difference parallel to the perturbation contours **E:** growing perturbation; **F:** decaying perturbation [Roos et al, 2004]

- The flow is accelerated by continuity in the cross-bank direction (perpendicular to the perturbation).
- The flow is slowed down by increasing friction due to a decrease in the waterdepth in along-bank direction (parallel to the perturbation).
- The flow is deflected by the Coriolis force.

These developments result in an along bank flow response that is transported downstream by advection. As this happens on both sides of the sandbank during one tidal cycle the net tidally averaged flow pattern is non-zero, resulting in a flow parallel to the bank contours. The sand conservation defines the growth of the perturbations as the depth increases due to net divergence of the sand transport leading to a net convergence of sediment at the crest. Depending on the orientation of the sandbank this causes the bank either to grow or decay. The bed evolution, in turn, affects the fluid motion, which affects the sediment transport, which affects the growth again, see figure 5. For the case of a 'finite' perturbation this residual flow will be deflected around it. Enhanced by the dominant deflection direction of the Coriolis force this will lead to a large circular flow over the perturbation and smaller flows on the flanks. The friction parameter causes the current coming of the perturbation to be retarded with regard to the reverse current approaching it, leading to a net on-bank sediment transport.

To determine which perturbations grow the fastest of all perturbations upon a bottom, Huthnance [1982] had to adopt a downhill preference of sediment transport. The assumption that sediment is more easily transported downhill was made to suppress the development of perturbations with a small mutual distance (wavelength), as those wavelengths are not in agreement with the dimensions of tidal sandbanks. The applied orientation and wavelength of the perturbations under which the bed evolves the fastest, is called the fastest growing mode.

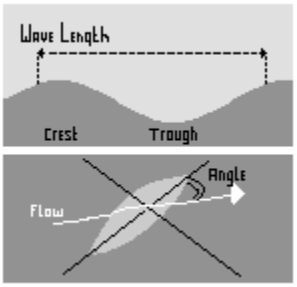

Figure 7: Wavelength and orientation

Having included a downhill preference Huthnance [1982] found that perturbations develop the fastest if their wavelength is between the 5 and 10km and if they have an orientation of 30° with respect to the direction of the tidal current. In addition he remarks that these results might differ under influence of coastline alignment or imposed increasing spacing of sandbanks because of increasing waterdepth along their length. As shown in paragraph 2.1 sandbanks and sand waves can be found at the same places. Nevertheless the appearance of sand waves next to sandbanks cannot be retrieved with Huthnance's model. Therefore Hulscher et al. [1993] adjusted the two dimensional model by implementing a parametric bed-load transport to represent the effects of the vertical current structure, which is not included explicitly in the model. Furthermore she allowed elliptical tides to occur which are a more realistic representation of the tide.

Although she found a critical mode for the formation of sandbanks, the model was not able to describe the co-existence of sand waves and sandbanks. Therefore Hulscher [1996] formulated a three dimensional flow model in which she explicitly defined the

vertical current structure, originated from changes in the horizontal flow velocity caused by friction variations of the sea-bottom. This inclusion leads to the formation of other sea-bottom features besides tidal sandbanks, like sand waves, due to the interaction of the basic current and the perturbed tidal components in the water column which generate residual currents.

When only looking at the development of sandbanks, the vertical distance over which changes in the horizontal flow due to friction can be noticed is of little importance. Hulscher [1996] therefore concludes that the formation of sandbanks can be described by depth-averaged models as Huthnance's [1982] or Hulscher et al.'s [1993]. The formation of sand waves can only be explained by three dimensional flow mechanisms and therefore not be explained through depth-averaged models. Furthermore she found that when only considering the growth of sandbanks the bottom friction has the largest impact on it if the wave vector, directed perpendicular to the sandbanks, makes an angle between 45 and 90° with respect to the mean stream. The Coriolis torque effects the growth the most if the wave vector is rotated 30 to 90° with respect to the main tidal current. Together these forces cause the largest growth if the wave vector is rotated at a maximum of 60°: the Coriolis force is dominant as the vertical stress is small.

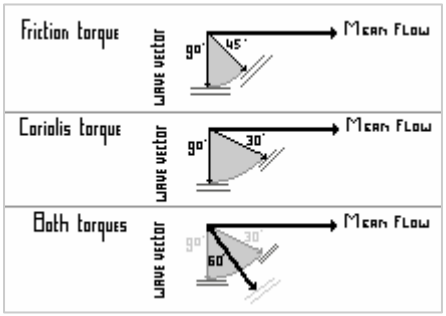

Figure 8: Wave vector against mean flow

As explained in section 2.1 a linear model can only describe the initial phase of sandbank development as the formation processes start to behave non-linear if the perturbations become larger. The development to their equilibrium shape, as we find them in nature, is therefore described through non-linear models and will be explained in the next section.

2.3.2 The Evolution towards equilibrium

Besides his research on the initial development of sandbanks, Huthnance [1982] also investigated the development towards equilibrium. An equilibrium could only be reached if there was a limitation to the available amount of sediment supply, which he implemented by placing the sandbank on a layer of non-erodable material. Within the development of the sandbank towards equilibrium he distinguishes the following phases:

1. Amplification of the initial sinusoidal perturbation.
2. Exposure of the hard layer which cannot be eroded and forms the limitation of the sediment supply, followed by contraction from the bank sides leading to vertical growth of the bank.
3. Development of the sandbank towards equilibrium: a flat broadened top and steep sides.

The time estimated by Huthnance [1982] in which the sandbanks would evolve to their equilibrium stage would be centuries.

Idier and Astruc [2003] also investigated the development of sandbanks towards equilibrium. The initial development of the sea bottom is determined by a linear analysis in which the instability depends on the velocity component parallel to the mean flow and the damping on the velocity in cross direction as well as the bottom slope effect. This result into a dominant mode: the mode which is growing the fastest, giving an indication on the wavelength and the angle of orientation. To determine whether a sandbank is already fully evolved, the growth rate of this mode is calculated for increasing values of the perturbation height: if the growth rate is zero the sandbank is said to be in equilibrium, if positive it is still growing and if negative, the applied height was overestimated. According to their numerical model based on a steady flow, the equilibrium height of sandbanks would be about 81% of the waterdepth, which is reached after 8,000 years approximately. They do think that their model makes an overestimation of the saturation height as data on sandbanks show a height between 56% and 71% of the waterdepth which could originate from various factors like, for example, the occurrence of storms.

This immediate comparison of the linear mode with the equilibrium height of the sandbanks might give a nice result according to Idier and Astruc's research [2003] but one should not think that the linear regime is capable of describing the final stage of sandbank formation. Nevertheless some improvements could be made in Huthnance [1982] model as was done by Roos et al. [2004]. They assumed a morphological evolution based on harmonic tidal flow components, bed-load and suspended-load transport and a depth dependent wave stirring term. This leads to a different development of the sandbanks towards their equilibrium shape independent of the amount of available sand supply. The first stage is the initial development within the linear regime, but as the perturbations become larger the processes starts to behave non-linear and during the second stage their sinusoidal shape is changed. The final stage is the development towards equilibrium. This behaviour is universal although unique for each applied wavelength and details might differ if model parameters are changed, for example:

- Bed-load sediment transport leads to spiky crests and flat troughs.
- Suspended sediment transport leads to sinusoidal shapes with lower flattened crests.
- The Coriolis force, bed friction and the slope coefficient have influence on the bank height and timescales.
- Tidal asymmetry, residual currents or wind waves affect the equilibrium height.

According to their model the equilibrium shape can have a height between 60% and 90% of the waterdepth. They also conclude that adopting a block-flow or steady flow is too crude to describe the development process of sandbanks towards equilibrium, as too little physics is captured.

So far all models discussed in this chapter are based on the assumption that sandbanks are instabilities within the morphological system, initiated by changes in the fluid flow due to perturbations in the seabed. There have been other approaches to explain the formation of sandbanks like that of Komarova and Newell [2000] as presented in the next paragraph.

2.3.3 A DIFFERENT APPROACH

The approach taken by Komarova and Newell [2000] is based on the non-linear development of sandbanks by sand waves. Their basic hypothesis is that sand waves are dynamically coupled so that the scale interaction of short scale waves triggers the formation of longer scale features i.e. sandbanks. Their model also uses the shallow water equations supplemented with a mass conservation law for the sediment transport. Their results show that the non-linear driving term for sandbanks is large enough to compete with the linear damping. The development of the seabed can now be seen as follows (see also figure 9):

(a) A current upon an unstable flat bed.
(b) The flat bed has evolved into perturbations with sandbank characteristics.
(c) Differences in sand properties lead to absence of troughs and crest at certain places.
(d) The overall mean level changes in which the flat areas form the top of the sandbanks.

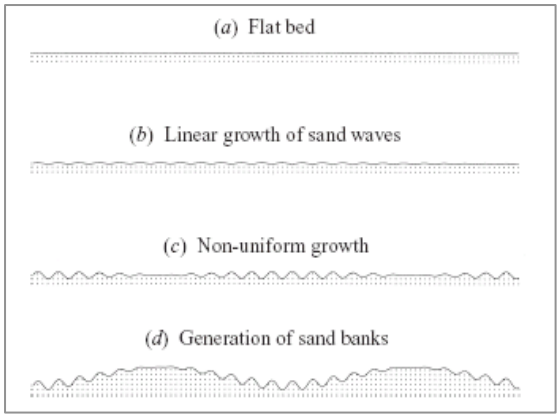

Figure 9: Formation of sandbanks out of sand waves [Komarova & Newell, 2000]

Although this model cannot be refuted there are reasons to question it in its present form [Vithana, 2002]: first of all it predicts that sandbanks will grow several meters in about 10 years, twenty times faster than the linear theorem, which is not in agreement with measurements. Secondly the model predicts an equilibrium height of about 5m although sandbanks as found in nature have a height in the order of 20 to 40m. Finally the orientation of the sandbanks differs compared to that of sand waves, which can not be explained by means of this model.

As the models based on the generation of sandbanks due to instabilities in the morphological system show good agreement with observations and are easier in use, preference is given to these models. Some applications of these models are discussed below.

2.3.4 APPLICATIONS

In 2002 Fluit and Hulscher combined the development of sandbanks with that of depressions due to gas mining. The induced depression changes the natural behaviour of sandbank formation. Distinction can be made between a system without or with sediment. In the former case the amount of subsidence depends on the distance to the centre of the depression. In the latter the subsidence follows the same pattern of evolution as the sandbank as the difference between the largest amplitude and his surrounding modes grows shifting towards a tidal sandbank mode. [Fluit & Hulscher, 2002]

The comparison between sandbank morphology and a subsidence (this time a sandpit) was further investigated by Roos and Hulscher [2003] to gain more knowledge on the effects of the implied seabed instability on the initial growth. Besides the development of the sandpit (deepening, deformation and possible migration) a sandbank pattern is formed, gradually growing, spreading and migrating around the pit. The overall conclusion of this research is the inherent instability of the flat bed: any pattern of perturbations on a sea bottom wants to develop into a pattern of cyclonic orientated banks. These developments are dependent on the strength of the Coriolis force, the local frictional effects and the pit depth.

2.3.5 DISCUSSION

Although the models developed so far can be used for practical purposes these models can not be seen as complete reflections of reality i.e. the morphodynamics of sandbanks is not completely covered yet. Problems that still need to be tackled are for instance [Roos et al, 2004]:

- Inclusion of the surface elevation during a tidal cycle, which would affect the bank heights negatively.
- Differences in the horizontal flow amplitudes in the top layers of the water column compared to those near the bottom as they are bend off by the Coriolis force.
- Adjustments for the sediment transport formula:
  Inclusion of a sediment transport threshold to be able to determine the total sediment transport (suspended as well as bed-load transport) instead of two separate estimations.
  Inclusion of grain size and relevant processes like hiding and exposure, as size variations might have an influence on the sandbank dynamics.
  Inclusion of changes in sediment supply which would result in changes of the sea floor elevation.

And in this paper the possible relation between sea level rise and the morphodynamics of sandbanks is under investigation. Why this relationship might exist will become clear in chapter 4, first the processes behind sea level rise will be explained in chapter 3.

3 SEA LEVEL RISE

Although Sea Level Rise (SLR) is often seen as a good indicator of climate change and studies in that context, it is also a feature of its own with associated specific problems as a result: inundation of land located below the sea surface, erosion of beaches and cliffs, salinization of aquifers and surface waters, corrosion of buildings and the environment and threatening of the lives of those living near the coast [Douglas, 1991]. These problems are serious but then again SLR has always been around. In this chapter the history of SLR is discussed, starting with a general description of SLR and its driving mechanisms followed by a more detailed study for the Southern Bight of the North Sea.

3.1 GLOBAL SEA LEVEL RISE

The sea level height in the past can be determined through the geological deposits it may left behind. Periods of high stand deposits fossils, glaucony or phosphorite, periods of fall may be retrieved in upward-shallowing successions and erosional unconformities [Hallam, 2001].

The periods of rise and fall describe time cycles with return periods of different length. So far the following cycles are retrieved:

1. Cycles with a period longer than 80 million years: corresponding broadly to the Palaeozoic (453-248 Million years Before Present (BP)) and Mesozoic –Cainozoic (248-0 Million years BP)
2. Cycles which lasted 10-80 Million years,
3. Cycles of 1-10 Million years,
4. Cycles of 40,000 to 100,000 years, corresponding to the Quaternary glaciations [Labau, 1995].

Since the 17th century the sea level rise in our area is stable with a variance between 0.1 to 0.24m per century [Douglas & Peltier, 2002]. This we know because of regular (daily) measurements, more precise data is collected from tide gauges (measuring devices) since 1933 [www.nodc.noaa.gov]. Although the tide gauges are well maintained by the responsible organisation (Permanent Service for Mean Sea Level) they take only local measurements of the relative sea level rise with respect to the solid earth. Furthermore it is difficult to gain long reliable records as tide gauges are subject to plate tectonic activities of the areas they are located in, like colliding plate boundaries, vertical variation due to volcanism, sediment compaction, fluid extraction or post-glacial rebound (PGR) [Douglas & Peltier, 2002]. PGR is the regional relaxation of the Earth's geoid where previous land-ice masses have melted. Without an independent estimation of vertical land movement it can not be determined whether the water level is rising, the land is sinking or both.

Figure 10: Tide gauge [www.imedea.uib.es]

It appears only gauge records of Western Europe and the Eastern United States are usable for determination of the Global Sea Level Rise (GSLR) as these areas are located on so-called passive continental margins i.e. no plate-tectonic processes are taking place there [Douglas, 1997]. Of these records only those with a record longer than 60 years and a completeness of 80% or more (of which the values are in agreement with the records of gauges in their surroundings) are usable. Besides the problem of correction for the vertical displacements of the earth the changes should also be placed in perspective to their source. Two sources can be distinguished:

- Steric rise: change in volume due to a change in sea water density by temperature change and salinity variations.

  Changes due to thermal expansion occur when the sea water expands or shrinks as the density changes by respectively a removal or addition of heat in both the deepest and surface layers of the oceans [Antonov, 2002]. Salinity also contributes to the expansion of the oceans, as larger concentrations of salt lead to a larger volume.
- Eustatic rise: change in volume by the exchange of water with the atmosphere or continents.

  The more common name for eustatic rise is ocean refreshening, which covers the total contribution of fresh water discharge (continental runoff including the melting of ice-masses) to the ocean [Munk, 2003]. Ocean refreshening is not a part of steric rise as the fresh water is colder than the salty water and its intrusion does cause growth in volume by a decrease in temperature but at the same time the salinity decreases, leaving the global volume unchanged.

If one wants to consider the total amount of increase of water over the Earth, corrections need to be made for the density of the water masses [Miller & Douglas, 2004]. In 1995 the Intergovernmental Panel on Climate Change (IPCC) published a sea level rise of 0.18 ± 0.01m per century for the past century, which was ascribed to steric processes. Levitus et al [2001] reported an increase of global ocean heat storage of the past 50 years which would on their own lead to a rise of 0.05m per century, leaving room for the eustatic contributions of 0.13 ± 0.01m per century. There is no consensus yet on the total amount of GSLR and as research continues other problems come to the surface like: the water stored in reservoirs and sinks, and changes in the groundwater level. [Douglas, 1997] This should also be taken into account if one wants to be precise on the estimation of the GSLR [Douglas & Peltier, 2002].

Most of the problems as presented above on the determination of the sea level are tackled if the area under consideration is smaller and one can make use of more detailed information. Therefore the specific case of the southern North Sea is discussed here.

3.2 THE SOUTHERN NORTH SEA

Paleozoic 354 – 251 million years ago	Carboniferous	(354 – 298 million years ago)
	Permian	(298 – 251 million years ago)
Mesozoic 251 – 65 million years ago	Triassic	(251 – 203 million years ago)
	Jurassic	(203 – 144 million years ago)
	Cretaceous	(144 – 61 million years ago)
Tertiary 65 – 2.6 million years ago		
Quatrain 2.6 – 0 million years ago	Pleistocene	(2.6 million – 10.000 years ago)
	Holsteinian	(410.000 – 370.000 years ago)
	Eemian	(130.000 – 115.00 years ago)
	Weichselian	(115.000 – 10.000 years ago)
	Holocene	(10.000 – 0 years ago)

Figure 11: Geological Time table

During the Carboniferous times a lot of crustal extension took place, which resulted into a basin that presently is known as the southern North Sea [De Mulder et al, 2003]. In early Westphalian times (305 – 318 million years ago) this area was still a foreland to a chain of Variscan Mountains that extended from south-west England through France into Eastern Europe. Subsidence of this area occurred in the early Permian, moulding it into a basin, which extended between eastern England and Poland, bounded in the north by the Mid North Sea High. Until the ending of the Triassic times the basin was a few times intruded by widespread transgressions of the Boreal Ocean. At the end of Triassic and beginning of Jurassic times, another crustal extension, this time with a north–south orientation, occurred, with crustal thinning the North Sea was pushed in its present NNW–SSE alignment. Ongoing subsidence, uplifting, erosion and sedimentation in the southern North Sea finally resulted in an enormous delta at the eastern side of a shallow to deep North Sea between 10 – 0.4 million years ago. As this delta was fed by Baltic rivers it had a western orientation. The Rhine, Meuse, Scheldt and some British rivers were becoming more important in the early Pleistocene, therefore the delta's orientation became more north–west. During the second half of the Pleistocene invasions of land ice occurred across the basin due to extreme changes in the temperature. Each subsequent warmer interglacial led to sea level rise and to the development of strong tidal, marine environments similar to those of the present. In the early Holsteinian interglacial period the rise in sea level re-established a shallow sea in this area, as did the interglacial period of the Eemian stage. The most recent glaciation is the Weichselian glaciation, in which the sea level fell to at least 110m below that of the present day [Jansen et al, 1983]. Once the Weichselian ice sheet began to decay, around 15,000 years ago, the sea level started to rise again. The earliest brackish water intrusion occurred 10,000 years BP when the sea level was 65m below the present value. The rise persisted and tidal sand ridges were formed west of the Dogger Bank, which became isolated to form a temporary island. The Southern Bight was connected with the northern North Sea as the land bridge flooded around 8,300 years BP, full marine conditions were not established before 7,000 years BP [Cameron et al, 1993].

The southern North Sea as we presently know it was formed from 9,000 years ago onwards. Earlier research on the bathymetry and sea level rise restricted itself to this period as will we. A further limitation is made for the bathymetry: we will only consider the Southern Bight of the southern North Sea, as the tidal sandbanks are located in that area.

3.2.1 SEA LEVEL RISE DURING THE PAST 9,000 YEARS

The southern North Sea is located south of the Dogger Bank and has a maximum depth generally not more than 50m. Samples for the estimation of the sea level over the past 9,000 years are gathered from the subsoil of the northern and the coastal plain of the Netherlands, Belgium and England. The first estimation made, showed a rapid rise in sea level at least since 8,000 years BP which gradually levelled since 6,000 years BP [Lambeck, 1989]. The estimation of a rapid SLR active at 8,000 years BP in the southern part and a change in rise about 6,000 years BP is in good agreement with the development of the bathymetry [Jelgersma, 1979]. The northern- and southern-part of the North Sea were separated by a land bridge 9,000 years ago. This bridge flooded between 8,500 and 8,000 years BP connecting the north with the south.

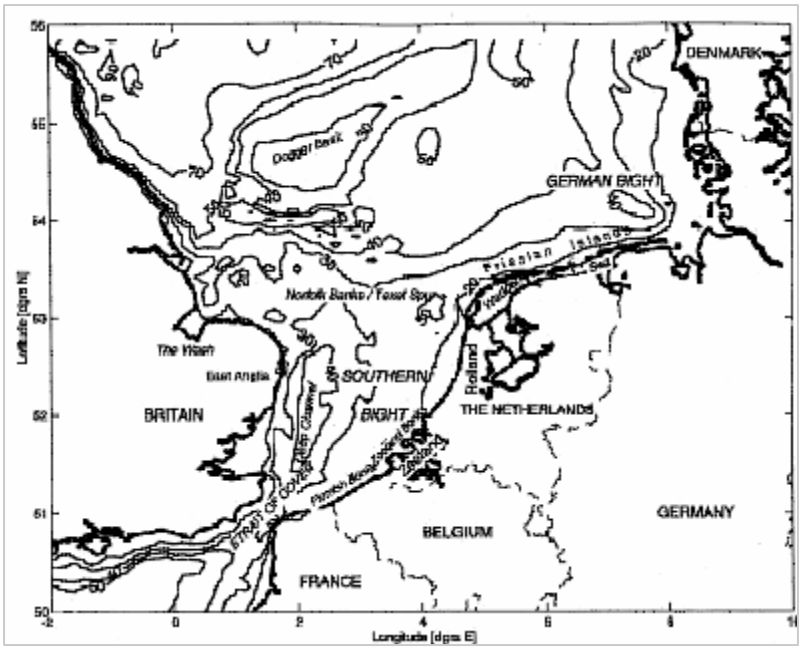

Figure 12: Southern Bight North Sea [Van der Molen, 1998]

The SLR initially proceeded at a rate of about 2m a century but slowed down considerably. This situation lasted until the North Sea was filled up 14m below the present level, today the SLR-rate is 0.15m a century. [Van Malde, 1996] These first estimations of SLR are based on eustatic processes only, as this could be retrieved in deposits. Van Dijck [1999] remarked that it was necessary to include corrections for compaction and subsidence due to relaxation. Relaxation is the redistribution of the Earth crust in response to the new distribution of the applied pressure until equilibrium is regained. During the last glacial period Scandinavia and surroundings was covered with ice and once that area started to unload the process of relaxation started. If the ice melts the pressure becomes less and the land is uplifted, at the same time the oceans fills giving more pressure on their floors leading to subsidence.

Beets and Van der Spek [2000] included these processes and estimated four possible paths for development of the relative sea level rise i.e. sea level rise in relation to land subsidence, over the past 9,000 years. Their distinction is based upon the different response to the relaxation of the areas they considered. The graph shows for all paths a gradually decline of the SLR-rate after 6,000 years BP from 0.7-1.6m to a ±0.1-0.3m per century. Based on their graph they claim that a small fall in SLR occurred between 5,500-4,500 years BP.

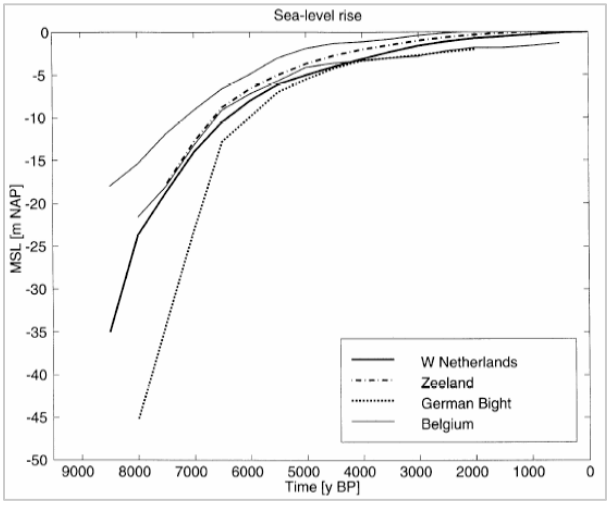

Figure 13: Relative sea level rises [Beets & Van der Spek, 2000]

As the development of the sea level differs for each location, Van der Molen and De Swart [2001] simulated the change for the entire southern part of the North Sea. When doing so they were also able to look at the dominating flow regime and the directions of the sediment transport. The actual development of the southern North Sea over the past 9,000 years adopted in this research is based on their simulation. Within this simulation three time periods stand out, which are discussed separately below. This chapter will end with a description of the present situation.

PERIOD 1: 9,000-8,500 YEARS BP

The first period covers the situation before flooding of the land bridge during which the SLR was the largest. In this period the southern part was dominated by a micro-tidal delta i.e. the influence of the tide is less than 2m, with two amphidromic points located in the Southern Bight and in the German Bight.

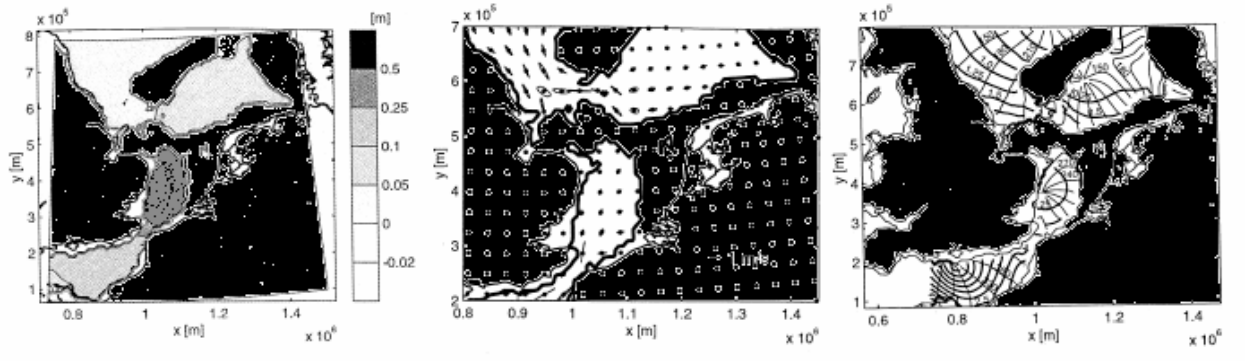

Figure 14: North Sea conditions 9,000 years Bp; *Left:* tide induced change in local mean sea level, *Middle:* current ellipses, *Right:* M_2-tide co-tidal charts. [Van der Molen & De Swart, 2001]

Most of the tidal energy entered the German Bight along the British east coast and entered the Southern Bight through the Strait of Dover. In the Southern Bight the elevations induced by the tide could reach a height of 0.5m above mean oceanic level.

Nevertheless the sediment transport was small during this period, directed onshore near the Netherlands but alongshore near Belgium. The dominant transport mechanism during this period was tidal asymmetry.

PERIOD 2: 8,500–7,000 YEARS BP

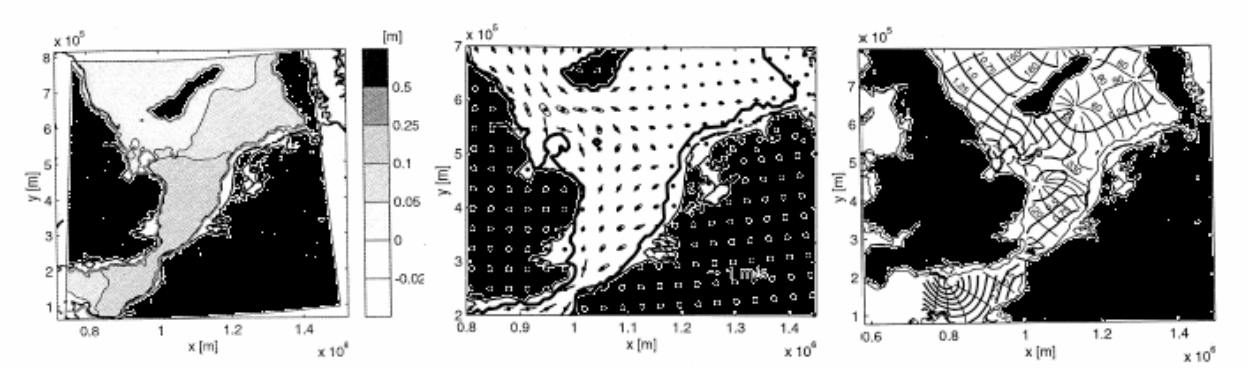

Figure 15: North Sea conditions 8,500 years Bp; *Left*: tide induced change in local mean sea level, *Middle:* current ellipses, *Right:* M_2-tide co-tidal charts. [Van der Molen & De Swart, 2001]

This period covers the development directly after the flooding of the land bridge. Because of drowning of the land bridge a tidal energy input was generated from the north to the south, leading to the formation of an amphidromic point in front of the coast of England. For a short period of time a residual current dominated the area after which it turned back to dominance by tidal asymmetry. The tidal amplitudes along the Belgian and southern Dutch coast had increased but were damped going south to north. The North Sea basin rapidly approached resonance as the waterdepth increased, leading to a fast increase of the dominant M_2 tidal amplitude. Furthermore the elevations of the sea level decreased and the difference in sea level with the oceans became less. The sediment transport increased substantially but the directions stayed the same. In the Southern Bight erosion took place as well as in the area of the former land bridge.

PERIOD 3: 7,000–0 YEARS BP

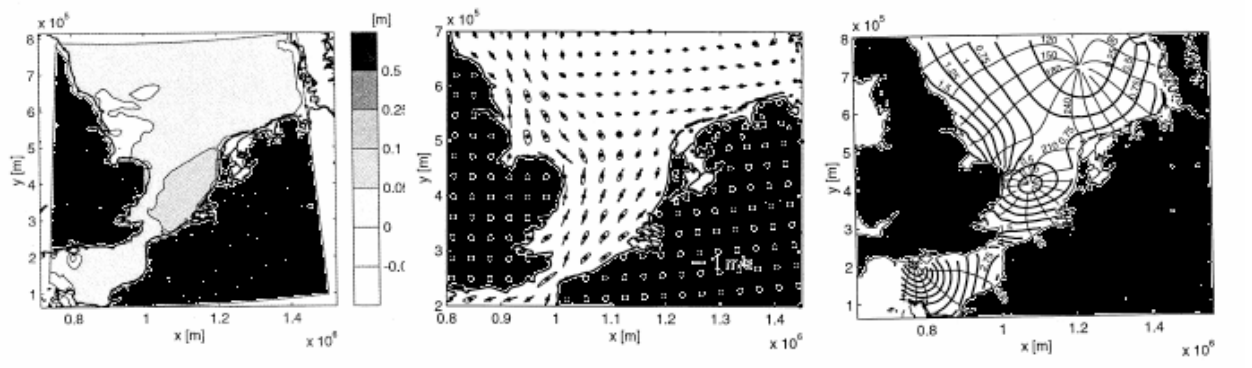

Figure 16: North Sea conditions 7,000 years Bp; *Left*: tide induced change in local mean sea level, *Middle:* current ellipses, *Right:* M_2-tide co-tidal charts. [Van der Molen & De Swart, 2001]

Under the continuing decrease in SLR-rate the land bridge was flooded ± 7,000 years ago, establishing the system as we presently know it. Aside from a delay in phase of the tide as the amphidromic point was still located slightly northwest of its present position resulting in larger tidal ranges along the western Dutch coast. The North Sea was dominated by a meso-tidal regime i.e. tidal range between the 2 and 4m. As the SLR-rate decreased since 7,000 years BP the development towards resonance decreased as well. The sediment transport in part of the Southern Bight changed direction to the south, creating a sand divergence zone. The Southern Bight was still dominated by erosion in the area of the former land bridge and by sedimentation due to northward alongshore transport along the Dutch coast.

PRESENT SITUATION OF THE NORTH SEA

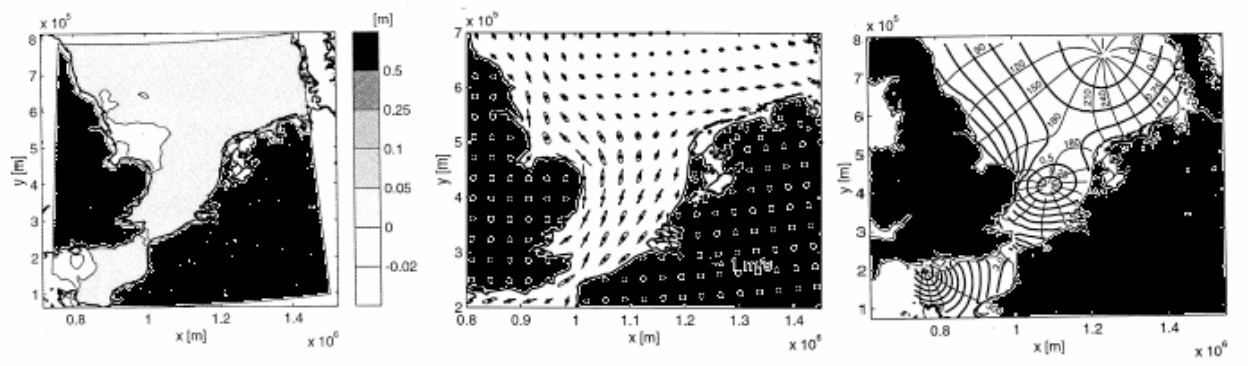

Figure 17: Present North Sea conditions; *Left*: tide induced change in local mean sea level, *Middle:* current ellipses, *Right:* M_2-tide co-tidal charts. [Van der Molen & De Swart, 2001]

Presently the North Sea is dominated by a circulation flow entering from the north from the Atlantic Ocean and leaving at Norway. With a surface of 54,000km^2 it is not large enough to have its own tidal current. The tides in the Southern Bight coming from the Atlantic Ocean are semi-diurnal, with dominant M_2 tidal amplitudes along the coast. In the Strait of Dover this tide can generate amplitudes of 2.4m but moving northerly it decreases towards 0.6m due to an increase of the bottom shear stress. In the Southern North Sea the sea bed consists mainly of fine to medium sands, whereas gravel can locally be found along the British coast and the Strait of Dover and silts and clays south of the Dogger Bank. As the dominant enforcing wind direction is from the northwest, the largest waves can be found in the north: the waves are about 18m in height and have a return period of 50 years. Southern waves are about 9m in height and have a return period of 10 years [Van der Molen & de Swart, 2001].

4 INFLUENCE OF SEA LEVEL RISE ON SANDBANKS

In chapter 1 it was stated that it is necessary to investigate the influence of sea level rise on the formation of sandbanks morphodynamics. Therefore the initial development of sandbanks and their further development towards equilibrium have been explained in chapter 2. This showed that their formation depends on a lot of different factors, but even under the most favourable conditions it takes centuries for a sandbank to develop. In chapter 3, sea level rise was discussed and as it shows this process changes the waterdepth enormously over centuries. To emphasize this statement the following calculation is performed:

A physical restriction to the formation of sandbank is the waterdepth; they can only be formed at places neither too deep nor too shallow. Let us state that after the flooding of the land bridge 8,000 years BP the waterdepth of the Southern Bight of the North Sea became deep enough for sandbanks to start developing. This assumption also clears the possible problems concerning the absence of sediment transport and the weak tidal system which occurred before 8,000 years BP. The following changes due to sea level rise occurred (based upon the average SLR over a period as estimated by Beets and Van der Spek [2000], section 3.2.1):

Period	Amount of centuries	Average SLR rate	Change in water level
8,000-6,000 years BP	20	$\left[\frac{1.6+0.7}{2}=\right]$ 1.15m per century	(1.15*20=) 23m
6,000-0 years BP	60	$\left[\frac{0.3+0.1}{2}=\right]$ 0.2m per century	(0.20*60=) 1215m
Total	**80**	**0.44m per century**	**35m**

Table 1: Sea level change past 8,000 years

As we can see in table 1 this would mean that the sea level has risen another 35m since. By personal communication with Dr. Schüttenhelm (2005) it became clear that this rise might be overestimated by at least 6m. The present depth of the former land bridge is about 29m and a surface erosion of several meters of the former land bridge area has to be assumed. On the other hand the uppermost layer of the seabed consists of one to a few metres of post-land-bridge sands. But as presently the deepest point in this area is about 65m, this still means that the depth has almost doubled since 8,000 years BP.

Nevertheless the models describing the morphodynamics of sandbanks assumed that the waterdepth has stayed constant over time. This is not a realistic representation of the development of the environment, and would never be even though the SLR-rate has slowed down to a present rate of 0.15 m a century.

This estimate shows why it is necessary to investigate the influence of sea level rise on sandbank morphodynamics.

5 MATHEMATICAL DESCRIPTION OF A LINEAR MODEL

In this chapter the mathematical background of a linear model describing the initial development of a sandbank as for the first time formulated by Huthnance [1982] is presented. The choice for conducting research in the linear regime is dual: the mathematics behind the linear models is simpler compared to that of the non-linear models and it forms the basis for beginning a non-linear analysis on sandbank development towards equilibrium. As this research is a first exploration of the influences of sea level rise on the sandbank formation, this possible connection shall be determined upon the occurrence of changes in the model output due to the implementation of different waterdepths. For this research the improved model of Huthnance [1982] by Hulscher et al. [1993] is used. By using this model insight in the influence of the waterdepth on the preferred sandbank characteristics consisting of the wavelength, the angle of orientation, the growth rate and the migration speed, can be gained.

5.1 MODEL FORMULATION

Within the linear regime different flow equations can be used to describe the morphodynamics which are: a steady flow*, an alternating block function† and a sinusoidal motion‡. As shown by Fluit and Hulscher [2002] the choice for one of these approaches hardly affects the linear results. For convenience the steady flow approach without time dependence of the flow is used. The area represented by the model is located far offshore so that it can be assumed that there are no influences of coastal alignment or changes in the waterdepth over the area. The tide dominates and no additional influences of waves are taken into account. The bottom shear stress is stated linear dependent of the main flow velocity, and only bed-load transport occurs for which no threshold is defined (which does not influence the model results as explained by De Vriend [1990]). Furthermore the wind stress at the surface is neglected.

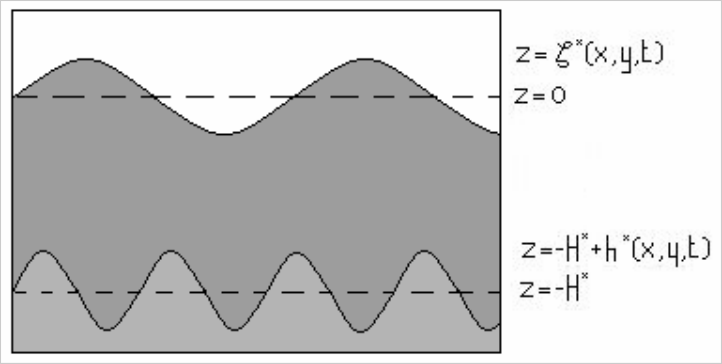

Figure 18: Sketch of offshore location

To describe the morphological development of the small perturbations placed on the bed the shallow water equations are used complemented with a formula combining the sediment transport with the seabed evolution, analogous to Hulscher et al. [1993] this reads:

* Steady flow: a flow with a constant velocity and direction over a time period.
† Alternating block function: a flow with a constant velocity, the direction of which becomes opposite in a period of time.
‡ Sinusoidal flow: the flow velocity and direction describe a sine pattern during a time period.

1. Momentum in x-direction:
$$\frac{\partial u^*}{\partial t^*}+u^*\frac{\partial u^*}{\partial x^*}+v^*\frac{\partial u^*}{\partial y^*}-f^*v^*=-g^*\frac{\partial \zeta^*}{\partial x^*}-\frac{r^*u^*}{H^*+\zeta^*-h^*} \qquad (5.1)$$
2. Momentum in y-direction:
$$\frac{\partial v^*}{\partial t^*}+u^*\frac{\partial v^*}{\partial x^*}+v^*\frac{\partial v^*}{\partial y^*}+f^*u^*=-g^*\frac{\partial \zeta^*}{\partial y^*}-\frac{r^*v^*}{H^*+\zeta^*-h^*} \qquad (5.2)$$
3. Mass balance of water:
$$\frac{\partial \zeta^*}{\partial t^*}-\frac{\partial h^*}{\partial t^*}+\frac{\partial}{\partial x^*}\left[(H^*+\zeta^*-h^*)u^*\right]+\frac{\partial}{\partial y^*}\left[\left(H^*+\zeta^*-h^*\right)v^*\right]=0 \qquad (5.3)$$
4. Formula combining the sediment transport and the seabed evolution
$$\frac{\partial h^*}{\partial t^*}+\vec{\nabla}^*\left[\alpha^*\left|\vec{u}^*\right|^b\left\{\frac{\vec{u}^*}{\left|\vec{u}^*\right|}-\lambda^*\vec{\nabla}^*h^*\right\}\right]=0 \qquad (5.4)$$

The u* and v* are the depth averaged velocity components in the x- and y -direction respectively, z=ζ* is the free surface elevation and h* is the bottom level with respect to the undisturbed bed level: z=-H* (figure 18). The x-axis is chosen in the direction of the principal current. Furthermore:

f*: Coriolis parameter

$f^*=2\Omega\sin\theta$ in which Ω = 2π/(24 hours) the angular velocity of the earth (often given in degrees per hour) and Θ in degrees the latitude on the earth.

g*: gravitational acceleration in ms^{-2},

r*: linearized friction parameter ($r^*=U^*C_D$,in which C_D is the drag coefficient and U* the tidal current amplitude in ms^{-1})

α*: sediment transport coefficient (this parameter includes the effect of porosity) in $\frac{m}{\left(ms^{-1}\right)^{b-1}}$;

b: power of transport (usually 3-5);

λ*: bed slope coefficient (usually of order 1-3)

As described in section 2.3.1 these equations form a closed system to describe the initial evolution of sandbanks. For convenience the parameters that hold dimensions are denoted with an asterisk (*), to be able to distinguish them with dimensionless parameters further down the mathematical analysis. To be able to solve the represented model it is convenient to non-dimensionalize the equations in search for very small parameters that can be neglected which makes the model simpler. For this procedure the following scaling is used:

$$\vec{u}=\frac{\vec{u}^*}{U^*};\qquad t=t^*\sigma^*;\qquad x=\frac{\sigma^*}{U^*}x^*;\qquad h=\frac{h^*}{H^*};\qquad \zeta=\frac{g^*}{U^{*2}}\zeta^*$$

in which:

- σ* is the tidal frequency in s^{-1},
- H* is the undisturbed waterdepth in m.

Performing the procedure results in:

$$\frac{\partial \zeta}{\partial x}+\frac{\partial u}{\partial t}+u\frac{\partial u}{\partial x}+v\frac{\partial u}{\partial y}-fv+\frac{ru}{1+\delta^2\zeta-h}=0 \qquad (5.5)$$

$$\frac{\partial \zeta}{\partial x}+\frac{\partial v}{\partial t}+u\frac{\partial v}{\partial x}+v\frac{\partial v}{\partial y}+fu+\frac{rv}{1+\delta^2\zeta-h}=0 \qquad (5.6)$$

$$\delta^2\frac{\partial \zeta}{\partial x}-\frac{\partial h}{\partial t}+\frac{\partial}{\partial x}\left[(1-h+\delta^2\zeta)u\right]+\frac{\partial}{\partial y}\left[(1-h+\delta^2\zeta)v\right]=0 \qquad (5.7)$$

$$\frac{\partial h}{\partial t}=-\alpha\vec{\nabla}\cdot\left\{\left|\vec{u}\right|^b\left[\frac{\vec{u}}{\left|\vec{u}\right|}-\lambda\vec{\nabla}h\right]\right\} \qquad (5.8)$$

Note that for all parts of the equations (5.5-5.8) to be dimensionless the new parameters formulated are:

$$\delta=\frac{U*}{\sqrt{g*H*}};\quad r=\frac{r*}{\sigma*H*};\quad f=\frac{f*}{\sigma*};\quad \alpha=\frac{U*^{b-1}}{H*}\alpha*;\quad \lambda=\frac{H*\sigma*}{U*}\lambda* \qquad (5.9)$$

It is necessary to distinguish between the time scales on which the hydrodynamic processes take place (an M_2 tide period takes about half a day) and the time scale of the morphodynamical processes (it takes sandbanks centuries to millennia to develop) as developments of the latter would not be noticeable on the time scale of the former. Therefore the morphological timescale is defined as: $\tau=\alpha t$. To decouple the hydrodynamics and the sediment transport from the bed evolution the quasi steady approach is used: omission of the fast bed changes $\partial h/\partial t$ in the water balance- and the sediment-equation. Although the fast bed changes are not taken into account during the tidal cycle, their average value during this period contributes to the long period evaluation of the sea bottom resulting in a tidal averaged (denoted by <>) sediment transport formula:

$$\frac{\partial h}{\partial \tau}=-\vec{\nabla}\cdot\left\langle\left\{\left|\vec{u}\right|^b\left[\frac{\vec{u}}{\left|\vec{u}\right|}\right]-\lambda\vec{\nabla}h\right\}\right\rangle \qquad (5.10)$$

Equations (5.5), (5.6), (5.7) and (5.10) form a dimensionless closed system through which the bed evolution can be calculated.

5.1.1 LINEAR STABILITY: THE BASIC STATE

When adopting the model of Hulscher et al. [1993] it is implied that sandbanks are formed as instabilities of a morphological system, section 2.3.1. To investigate whether or not this is true it is necessary to define a basic state: a tidal current upon a flat bottom. To determine if this state is stable, small perturbations are placed upon it. The basic state is stable if all these perturbations decay, complementary [Hulscher et al, 1993]: if there is at least one perturbation with a positive growth rate the basic state is unstable.

Mathematically the solution of the problem can be symbolically written as the vector containing the four variables of the problem:

$$\phi = \left(\hat{u}, \hat{v}, \hat{\zeta}, \hat{h}\right) \tag{5.11}$$

The spatially uniform but time independent state which is a solution to equations (5.5) – (5.7) and (5.10) is:

$$\phi_0 = (u_0, v_0, \zeta_0, 0) \tag{5.12}$$

Analogous to Hulscher et al. [1993] the amplitude of the perturbation with respect to the undisturbed waterdepth is denoted by μ, expanding (5.11) in power series of μ results in an approximate solution:

$$\phi \approx \phi_0 + \mu\phi_1 + \mu^2\phi_2 + \ldots$$

Only the linear solution is relevant thus higher order terms in μ can be neglected. To be able to neglect the contribution of the free surface elevation ($\partial\zeta^*$) to the waterdepth, the rigid lid approach is adopted. Closing the procedure by taking the derivative of μ for each part of the equation and substituting μ = 0 for those parts that still include a μ, we arrive at the following system:

$$\frac{\partial\zeta_1}{\partial x} + \frac{\partial u_1}{\partial t} + u_0\frac{\partial u_1}{\partial x} + v_0\frac{\partial u_1}{\partial y} - fv_1 + ru_0h_1 + ru_1 = 0 \tag{5.13}$$

$$\frac{\partial\zeta_1}{\partial y} + \frac{\partial v_1}{\partial t} + u_0\frac{\partial v_1}{\partial x} + v_0\frac{\partial v_1}{\partial y} + fu_1 + rv_0h_1 + rv_1 = 0 \tag{5.14}$$

$$-u_0\frac{\partial h_1}{\partial x} + \frac{\partial u_1}{\partial x} - v_0\frac{\partial h_1}{\partial y} + \frac{\partial v_1}{\partial y} = 0 \tag{5.15}$$

$$\begin{aligned}\frac{\partial h_1}{\partial\tau} &+ \frac{\partial}{\partial x}\left[\left|\vec{u_0}\right|^{b-1}u_1 + (b-1)\left|\vec{u_0}\right|^{b-3}u_0\left(u_0u_1 + v_0v_1\right) - \left|\vec{u_0}\right|^{b}\lambda\frac{\partial h_1}{\partial x}\right] \\ &+ \frac{\partial}{\partial y}\left[\left|\vec{u_0}\right|^{b-1}v_1 + (b-1)\left|\vec{u_0}\right|^{b-3}v_0\left(u_0u_1 + v_0v_1\right) - \left|\vec{u_0}\right|^{b}\lambda\frac{\partial h_1}{\partial y}\right] = 0\end{aligned} \tag{5.16}$$

This system describing the bottom evolution h_1 can de solved by Fourier-transforming the unknowns, u_1, v_1, h_1, and ζ_1 in the equation-set (5.12), (5.13) and (5.14) with:

$$\phi_1 = \left(\hat{u}_1, \hat{v}_1, \hat{\zeta}_1, \hat{h}_1\right)e^{i\mathbf{k}\cdot\mathbf{x}} + c.c. \tag{5.17}$$

Here $i^2 = -1$, c.c. stands for the complex conjugate and, $\mathbf{k}$ = (k, l) is a two-dimensional wave vector. Besides that Fourier-transforming the variables gives a solution for the bottom evolution it also tells how the perturbations are placed upon the flat bottom. To determine their orientation with regard to the main flow the angle between them can be determined through:

$$\textit{angle of orientation} = \arctan\left(\frac{k}{l}\right) \tag{5.18}$$

And their wavelength by:

$$wavelength = \frac{2\pi U^*}{K\sigma^*} \tag{5.19}$$

In which K is the length of the dimensionless wave vector:

$$K = \sqrt{k^2 + l^2} \tag{5.20}$$

By Fourier-transforming the unknowns (knowing that the bottom topography is an infinite domain which can be decomposed in a unique way into a spectrum of wave components) the integration of these wave components exactly equals the bed topography. The transformation leads to a complete linear system in which the time dependent terms $\frac{\partial u_1}{\partial t}$ and $\frac{\partial v_1}{\partial t}$ can be neglected and the result is combined in the matrix equation:

$$\begin{bmatrix} (u_0 il + v_0 il + \hat{r}) & -f & ik \\ f & (u_0 ik + v_0 il + \hat{r}) & il \\ ik & il & 0 \end{bmatrix} \begin{bmatrix} \hat{u}_1 \\ \hat{v}_1 \\ \hat{\zeta}_1 \end{bmatrix} = \begin{bmatrix} -\hat{r}u_0 \\ -\hat{r}v_0 \\ (u_0 ik + v_0 il) \end{bmatrix} \hat{h}_1 \tag{5.21}$$

The bed evolution of the system is found by solving the matrix equation (5.21) and inserting the results in the bottom evolution equation (5.16) resulting in:

$$\left\{ \frac{\partial \hat{h}_1}{\partial t} = \alpha\omega\hat{h}_1, \quad \hat{h}_1\Big|_{t=0} = h_{Init} \right\} \Rightarrow h(t) = h_{Init} e^{\alpha\omega t} \tag{5.22}$$

In which the parameter ω is a complex quantity given by:

$$\omega = |u_0|^b ik \left[\frac{br\left(l^2 - k^2\right) + fkl\left(1 - b\right) - iu_0 k\left(bk^2 + l^2\right) - 2l^2 r}{\left[il^2 u_0 k + iu_0 k^3 + r\left(k^2 + l^2\right) \right]} \right] - \lambda |u_0|^b \left(l^2 + k^2\right) \tag{5.23}$$

With the formula for bed evolution the development of the perturbations can be determined. Whether or not this result in a decay or growth of the features depends on the sign of the growth rate, which is now in dimensional form determined as:

$$Growthrate = \varpi_{\mathrm{Re}} \alpha\sigma^* \tag{5.24}$$

In which the real part of omega (equation 5.23) is:

$$\omega_{\mathrm{Re}} = k\left(k^2 + l^2\right) \left[\frac{-u_0 k\left(k^2 b + l^2 - br\left(l^2 + k^2\right) + fkl\left(b - 1\right) + 2lr\right)}{\left(-rk^2 - rl^2\right)^2 + \left(-l^2 u_0 k - u_0 k^3\right)^2} \right] - \lambda\left(k^2 + l^2\right) \tag{5.25}$$

If the sign of the growth rate is negative, the features will decay and if it is positive the perturbations grow. Earlier research, see section 2.3.1, has shown that for certain values of the two dimensional wave vector, the perturbation has a positive growth rate. Which features develop, under which angle and with which wavelength, depends is contained in the mode which has the largest growth rate.

This mode is called the fastest growing mode and the features grow exactly according to an e-folding timescale (equation 5.22). The last sandbank characteristic which can be determined within the linear regime is the migration speed: the speed with which the features move in the flow direction. The migration speed can only be found if there is a residual flow in a certain direction i.e. if a symmetrical alternating block flow or symmetric sinusoidal flow was considered, this sandbank characteristic could not have been calculated. In dimensional form the calculated is as follows:

$$Migrationspeed = \frac{-\omega_{Im}\alpha U^*}{K} \tag{5.26}$$

In which ω_{Im} is the imaginary part of ω (equation 5.23) defined as:

$$\omega_{Im} = k\left(k^2 + l^2\right)\left[\frac{-br^2\left(l^2 - k^2\right) + fklr\left(b+1\right) + 2lr^2 + u_0^2k^2\left(-bk^2 - l^2\right)}{\left(-rk^2 - rl^2\right)^2 + \left(-l^2u_0k - u_0k^3\right)^2}\right] \tag{5.27}$$

Together the angle of orientation, the wavelength, the growth rate and the migration speed give an indication on the preferred development of the sandbanks within the linear regime. To determine if there is a connection between sea level rise and the development of sandbanks the effect of changes in the waterdepth on these sandbank characteristics is investigated.

6 Methodology for conducting a Sensitivity Analysis

The investigation of the influence of changes in the sea level on the fastest growing mode is called a sensitivity analysis, which here can be generalised into: the investigation of the sensitivity of the model describing sandbank morphodynamics to changes in a certain parameter within this model. According to Jansen et al. [1990] the standard procedure to perform such an analysis is:

1. Formulation of the research objective.
2. Specification of the parameters which are to be varied within the sensitivity analysis.
3. Specification of the basic value and the variation applied to these parameters.
4. Performing the analysis.
5. Conducting a robustness analysis on the results in order to determine how insensitive the results are with regard to the choices made.

This chapter deals with the first four items. In chapter 7 the results are presented in graphs and placed in perspective to their physical background. The results of the sensitivity analysis are placed in perspective to the limitations of the model and method used within this research in chapter 8. The robustness analysis forms a part of chapter 8. Before in the final chapter the overall conclusions are drawn, a comparison with reality is made in chapter 9.

6.1 Research Objective

To determine the influence of sea level changes on the initial development of sandbanks by means of a linear model, changes in the sandbank characteristics as a result of different waterdepths are investigated. If the outcome for each waterdepth are put together in one graph the change within one of the preferred sandbank characteristics against increasing waterdepth can be determined. Based on this, the research objective as given in chapter 1 can be rephrased in more detail as:

How do different values for the waterdepth affect the preferred sandbank characteristics?

6.2 Parameter specification

As the process of sea level rise covers more than just a change in the waterdepth, see chapter 3, it is of importance to determine if changes in other input parameters could have occurred over time as well. This is done for each parameter separately below.

The Flow velocity

In section 3.2.1 it was shown that it took time for the present M_2 tidal mechanism to establish, therefore it is not realistic to assume the flow velocity constant over time. A more realistic approach could be assuming the water flux (H^*U^*) constant over time as the total amount of water flowing in and out of the North Sea is more stable, but than changes in the bathymetry are not taken into account. The real development of the flow velocity lies probably in between either of the two approaches and therefore both approaches are performed.

The Tidal frequency

In section 3.2.1 it is shown that except for a short period of time the M_2 tide dominated the North Sea. Therefore this parameter (σ^*) can be considered a constant.

The Coriolis parameter

The deflection caused by the Coriolis force depends on the latitude (θ), see section 2.3. The southern North Sea covers a large area matching with different latitudes. As a difference in the latitude leads to a difference in the Coriolis force, it is taken into account.

The drag coefficient

The standard variation in the applied drag coefficient (C_D) for shallows seas is between the 0.01 and 0.001. As the friction of the North Sea sea-bottom has not stayed constant over time, section 3.2.1, and is defined as: $r^* = C_D U^*$ changes in the drag coefficient are taken into account.

The Transport formula power

The power of the transport formula (b) is usually chosen between 3 and 5. This power reflects the faster than linear dependency of sediment transport on the flow velocity. As no physical coupling exists for this parameter, it is said to stay constant over time.

THE SEDIMENT TRANSPORT COEFFICIENT α

It is stated that the constant α represents the porosity, section 3.2.1, but to be precise this parameter also stands for a small contribution in the friction as well. It represents together with the nonlinearity parameter b the efficiency of the particles of sand that are transported by the bed shear stress. Variations in this parameter are not taken into account as its influence is very easy to retrieve: if α becomes a factor x as large, the development of the morphology would go a factor x as slow according to: $\tau = \alpha t$.

THE SLOPE FACTOR

The slope factor (λ^*), also known as the bed slope coefficient, describes the downhill preference of moving sediment. The downhill transport depends on gravity, flow shear stress as well as the weight of the sediment particles [Komarova & Hulscher, 2000]. As the composition of the sediment could have changed over time, different values for the slope factor are taken into account.

Having discussed each parameter of the above presented list, the conclusion can be drawn that it is not necessary to take changes in the tidal frequency, the power exponent and the sediment transport coefficient into account. As variations in the value of the other parameters might have occurred during the past 9,000 years a sub-research question is formulated to determine their influence on the sandbank formation as well:

How do variations in the values of the flow velocity, the water flux, the latitude, the drag coefficient and the slope parameter influence the results of the main objective?

To be able to give a good impression on the change in development of the sandbanks during the time in which they were formed, the possible variation in the value of the parameters needs to be defined. Presently the typical values for the input parameters are [Fluit & Hulscher, 2002]:

- A flow velocity (U^*) of the dominant North Sea M_2 tide of 1 ms^{-1}.
- A water flux (H^*U^*) of 30 ms^{-2} (based upon the typical assumed depth of 30m).
- A frequency (σ^*) of the M_2 tide of 1.4 x 10^{-4} s^{-1}.
- A Coriolis parameter (f^*) at a latitude (θ) of 52°N is 1.15 x $10^{-4}s^{-1}$.
- A drag coefficient (C_D) in the North Sea lies between 0.01 and 0.001, here chosen at 0.0055.
- A gravitational acceleration (g^*) of 9.81 ms^{-2}
- A transport formula power (b) of 3 leading to a sediment transport coefficient (α^*) of 1.5 10^{-5} s^2m^{-1}, according to Van Rijn [1993]
- And the slope factor (λ^*) is set equal to 2.

To determine the maximum additional influence of the parameters which did most likely not stayed constant over the past 9,000 years the extremes values that could have occurred are determined for each parameter individually below. The basic value for each parameter is the typical value as presented above.

6.3 VARIATION IN PARAMETER VALUES

As the variations in the input parameters are used to investigate the possible deviation in sandbank formation of tidal sandbanks located in the southern North Sea, the applied extreme values are representative for this area.

THE WATERDEPTH

The present depth variation in the southern North Sea is between 20 and 55m (figure 19). The basic value chosen for the North Sea depth (H^*) is 30m [Fluit & Hulscher, 2002]. The variation chosen for the waterdepth is from 10 to 65m. The choice for the lower boundary is based upon the condition that the waterdepth needs to be sufficient deep for sandbanks to develop. The upper boundary matches the condition that sufficient strength in the current is necessary for sediment transport to occur which leads to bed evolution. Furthermore is the assumption of a depth averaged flow velocity for larger waterdepths than 65m not realistic.

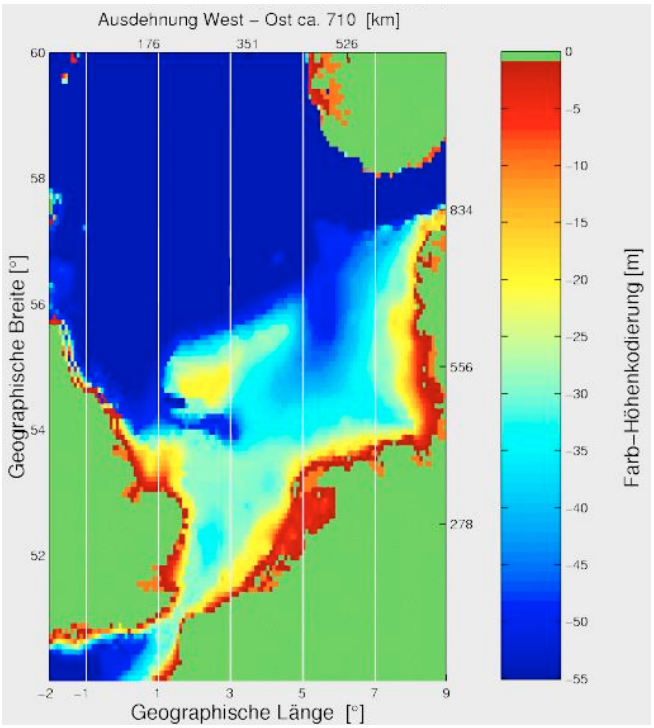

Figure 19: Waterdepths in the North Sea [www.noordzee.org]

THE FLOW VELOCITY

The present range in the flow velocity (U^*) for the southern North Sea is 0 to 2.0ms^{-1}. Because very weak flow velocities are unable to transport sufficient sediment the lowest value chosen for the flow velocity is set at 0.83ms^{-1} (5/6 of 1.0ms^{-1}). The highest value is set at 1.16ms^{-1} (7/6 of 1.0ms^{-1}) to get an similar range around the average value of 1.0ms^{-1} and a first indication of the possible influence of changes in the flow velocity on sandbank formation. As the most commonly chosen waterdepth value is 30m belonging to 1.0ms^{-1} flow velocity, the water flux (H^*U^*) variation is set at 25m^{2}s^{-1} (5/6 of 30m^{2}s^{-1}) and 35m^{2}s^{-1} (7/6 of 30m^{2}s^{-1}). By adopting the same range in values it is possible to compare of the influence of both approaches on sandbank formation to each other.

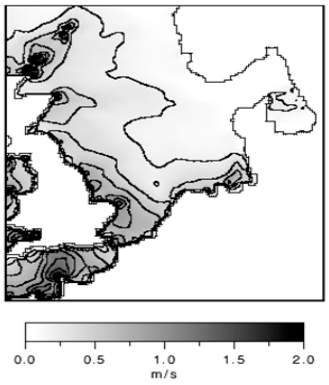

Figure 20: Flow velocities in the North Sea [www.noordzee.org]

THE LATITUDE

The standard value for the latitude (θ) taken for the southern North Sea is 52° northern latitude. The value for the latitude is varied over: 51 (low value), 52 (basic value) and 53° northern latitude (high value), in accordance with its location.

THE DRAG COEFFICIENT

According to Fluit and Hulscher [2002] the drag coefficient (C_D) for shallow seas lies between the 0.01 (high value) and 0.001 (low value) which therefore form the maximum and minimum value applied in this research. The basic value is chosen at $C_D = 0.0055$ (section 6.3).

THE SLOPE PARAMETER

The standard variation allowed for the slope parameter (λ^*) is between 1 (low value) and 3 (high value) [Hulscher et al, 1993, Fluit & Hulscher, 2002] which is adopted here. The basic value for the slope parameter is set at 2.

6.4 ANALYSIS PROCEDURE

Before the analysis can be performed the method used needs to be explained. To determine the influence of the waterdepth on sandbank characteristics all other parameters are taken constant at their basic value. For each change in waterdepth, with a magnitude of 10 cm, the fastest growing mode is numerically obtained. To determine the fastest growing mode within the area under consideration a numerical process is defined in MAPLE. This model systematically goes trough all possible combinations of the wave vector components within a certain limited area, to the detail of 1000^{th}, to determine the combination with the largest real part of omega. To make sure that for each waterdepth a maximum was found the numerical process was broadened if the mode lay on a boundary. Once the fastest growing mode was determined, the imaginary part of omega can be calculated as well. Based on this output the growth rate, the wavelength, the angle of orientation and the migration speed were determined in EXCEL and put together in a graph. Ergo each graph represents the development of a sandbank characteristic against increasing waterdepth.

Within this calculation procedure distinction is made between a constant flow velocity approach and a constant water flux approach, as the flow velocity is directly connected to the waterdepth. Besides that for both approaches the development of the sandbank characteristics against increasing waterdepth is calculated, the additional influence of changes in one of the other parameters (drag coefficient C_D, slope factor λ^* and latitude θ) is calculated as well. The investigation into the additional influences of the other parameters on the development of sandbanks under an increasing waterdepth can be seen as a robustness analysis as it gives an indication of how (in)sensitive the development is to the value-choices made for the other parameters.

The graphs representing the changes in the sandbank characteristics for both approaches are given in the next chapter. The additional influences due to changes in the value of another parameter are recorded in the appendixes but will be discussed as well.

7 RESULTS

This chapter deals with the results from the numerical procedure and puts them in the perspective of their physical background. This is done for each sandbank characteristic. In the next chapter an overall discussion on the found results comparing them to each other by means of a robustness analysis is given.

7.1 GROWTH RATE

For both approaches an increase in the waterdepth leads to a decrease in the growth rate. This can partly be explained by equation 5.24: the constant α is proportionally decreasing with increasing waterdepth (equation 5.9). Because α also depends on the flow velocity, the growth rate found by applying a constant water flux has a much higher value for shallow water and much smaller values at deeper water compared to the constant flow velocity approach.

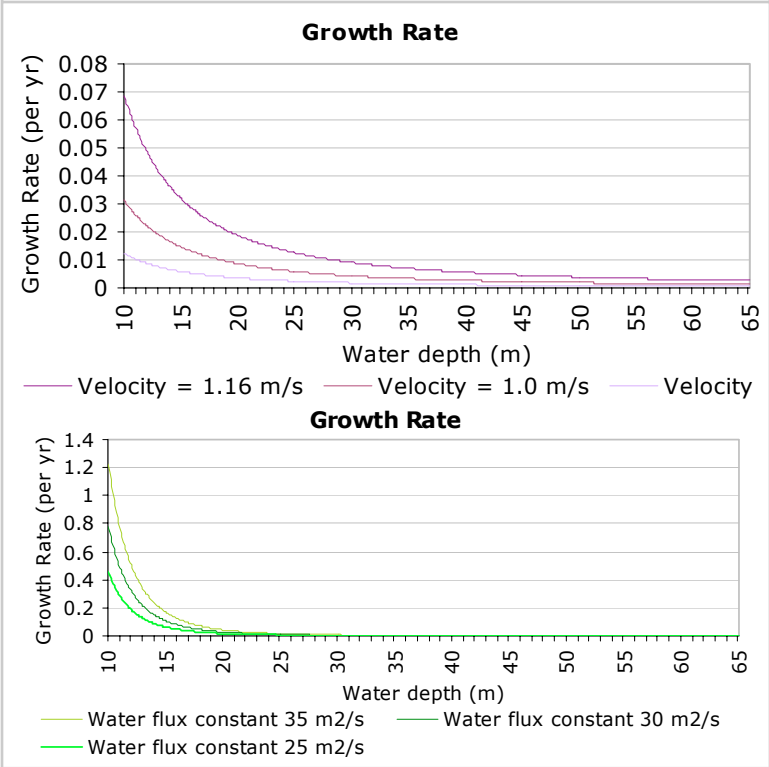

Figure 21: Growth rate against waterdepth
Upper: constant flow velocity
Lower: constant water flux

The other part is determined by changes in the fastest growing mode: the fastest growing mode may shift when considering a different value for the waterdepth. In appendix A the changes in the development of the growth rate when varying other parameters are presented. As the first graphs show: larger values of the drag coefficient lead to larger growth rates. This is consistent with the linearized friction parameter: $r = \frac{C_D U^*}{\sigma^* H^*}$ in which the drag coefficient is located in the numerator i.e. when keeping all other parameters constant, a larger value of the drag coefficient (C_D) would immediate lead to a larger value of the friction. Apparently the implementation of the linearized friction parameter in the real part of omega (equation 5.25) is such that this leads to larger growth rates as well. This is also physically explainable: the larger the friction of the sea bottom the larger the retardation of the current coming of the sandbank is, compared to a situation with a lower friction. The graphs representing the changes made in the slope parameter (λ^*) value shows an opposite development: the larger the value the smaller the growth rate.

This can directly be concluded from equation 5.25 in which the slope parameter has a negative contribution to the growth rate, for all values of k and l. Physically interpreted, the slope parameter represents the downhill preference of the sediment particles and if this preference is larger i.e. the slope parameter is larger, the growth rate will become smaller as the perturbation will develop less steep. The influence of changes in the latitude (θ) is not noticeable for the applied variation.

7.2 ANGLE OF ORIENTATION

The North Sea is located in the Northern Hemisphere, in which the Coriolis force deflects the currents to the right and to get positive values for the angle of orientation it is presented counter clockwise. As figure 22 shows, the angle is increasing with increasing waterdepth for both approaches, although a different path is described: the path of the constant flow velocity is almost straight whereas the path of the constant water flux approach is clearly curved. Furthermore the angle of orientation stays smaller under the constant flow velocity approach and has a constant difference in angle between the applied velocities, in contrast to the graph of the constant water flux approach.

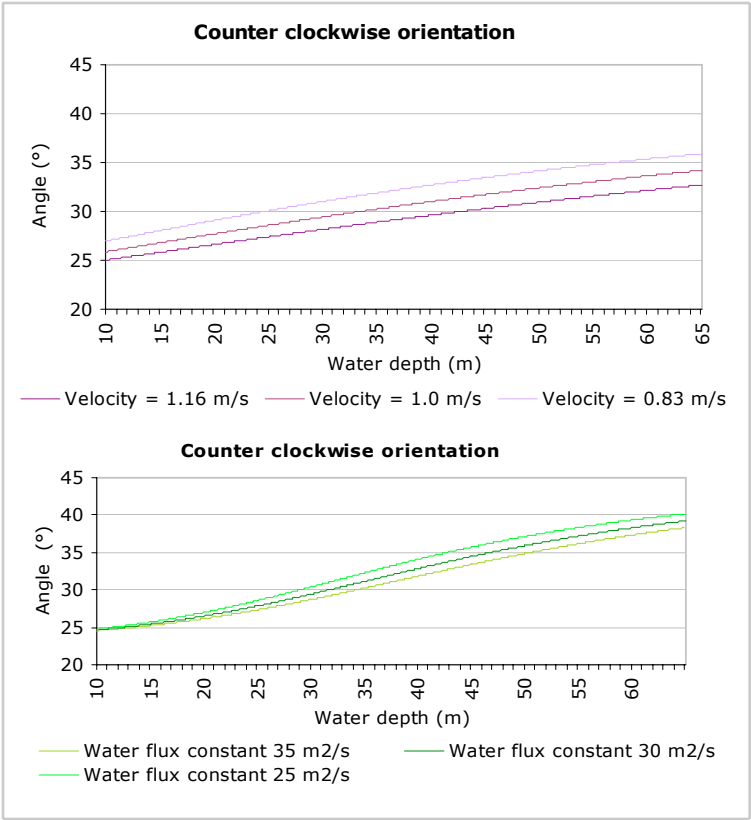

Figure 22: Counter clockwise orientation against waterdepth
Upper: constant flow velocity, *Lower*: constant water flux

Apparently is the development of the fastest growing mode the same for different values of the flow velocity only starting at another value, whereas the development is different for different values of the water flux (as the lines overlap at shallower depths). The fact that the angle of orientation is larger for larger values of the flow velocity (also in the constant flux approach) can be deduced from the linearized friction parameter: as the friction increases with increasing flow velocity (section 7.1) the angle between the current and the flow velocity decreases as a dominant friction force matches smaller angles of orientation (section 2.3.1). In appendix B this development is also shown for changes applied to the drag coefficient (C_D): smaller angles match with larger values. The crossing of different paths is most likely the change in dominance from the Coriolis force to the friction parameter, which affects the angle (section 2.3.1).

The influence of the friction is also noticeable through the slope factor (λ^*). The larger the downhill transport the less steep the sandbanks are, referring to section 7.1, resulting in less friction on the water column. According to section 2.3.1 a smaller friction force matches with larger angle of orientation, corresponding to figure 30. Similarly decreasing values of the Coriolis force match with larger angles of orientation (differentiating from the influence of the friction, that these angles can become much larger, see figure 8). Unfortunately this can not be retrieved in the graphs shown in appendix B, as the applied variation is apparently too small.

7.3 WAVELENGTH

Although the wavelength is increasing with increasing waterdepth, both approaches show a different range in the developments. Looking at equation 5.19 it is obvious to conclude that an increasing value of the flow velocity would lead to an immediate increase of the wavelength. But the influence in the development of the dimensionless wave vector (K, equation 5.20) also has a large influence on the development of the wavelength, as an increase in the wavelength against increasing waterdepth can only originate from an decrease in K (all other parameters are after all constants).

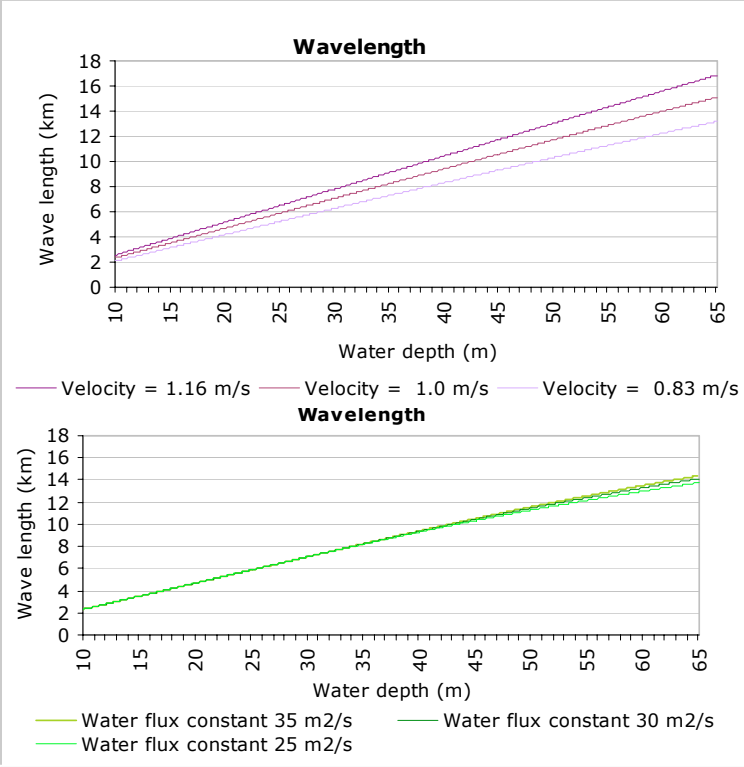

Figure 23: Wavelength against waterdepth for both approaches

For the lines describing a constant water flux to overlap, the differences in the flow velocity at a certain waterdepth has to be compensated by the same difference in the value of K. Furthermore, with reference to section 7.2, the wavelength also depends on the amount of bottom friction. This is decreasing faster for the constant water flux approach as not only the waterdepth decreases but also the flow velocity. The influence of the drag coefficient (C_D) and the preferred downhill transport is also shown in graphs in appendix C. Analogous to section 7.2: a larger value of the drag coefficient leads to more flow retardation and therefore a faster growth with overall smaller wavelengths. A larger slope factor (λ^*) also leads to slower growth of the features and therefore to larger wavelengths. For the Coriolis force the influence would be opposite (smaller values for higher latitudes), which cannot be seen in the appendix as the variation in its value is too small.

7.4 Migration Speed

The development of the migration speed seems similar to that of the growth rate and follows the same path for both approaches: decreasing with increasing waterdepth. Looking at equations 5.24 and 5.26 the following similarity can be found: a decrease in the parameter α with increasing waterdepth, which is increasing faster for the constant water flux approach. As the flow velocity is also in the numerator of equation (5.26) the influence of the flow velocity is larger for the migration speed compared to the growth rate. This would explain the overall smaller value for the constant flow velocity and overall larger value for the constant water flux approach, compared to the growth rate. The only parameter contradicting this development is the dimensionless wave vector (K), which is increasing with increasing waterdepth. Apparently this does not affect the declining path of the migration speed.

Besides these obvious differences, the differences in the real part and imaginary part of omega should be taken into account as well. Therefore no direct relation can be drawn between these two sandbank characteristics.

Applied variations in the other parameters are represented in appendix D. It shows that only the drag coefficient (C_D) has influence on the development of the migration speed; especially for the constant water flow approach.

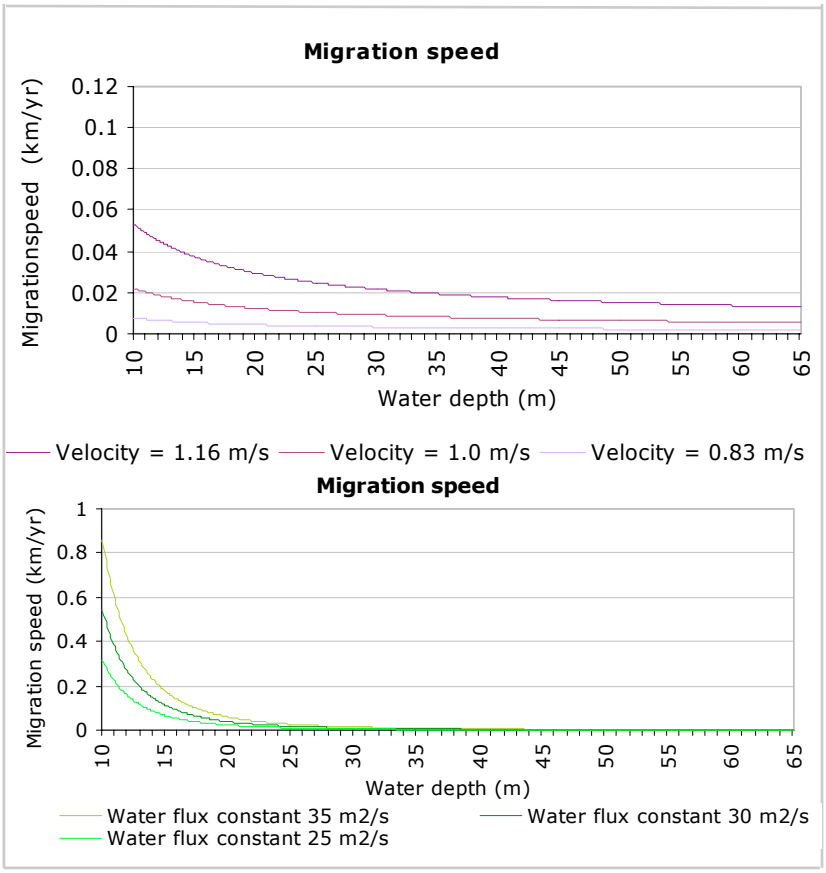

Figure 24: Migration speed against waterdepth; *Upper*: constant flow velocity *Lower*: constant water flux

This is not surprising as the slope parameter (λ^*) is not a part of the imaginary part of omega (equation 5.27) and so far the applied changes in the latitude (θ) have not shown any deviance in one of the characteristics. The drag coefficient is included in the imaginary part of omega by the linearized friction parameter. Apparently these changes lead to little variation in the imaginary part of omega compared to the larger changes in the parameters α and K.

8 DISCUSSION

Before the overall conclusions which are based on the results found through this research can be drawn, the advantages and disadvantages of the used methodology and model are discussed in this chapter. A proper way to determine if the used method was suitable is by means of a robustness analysis (chapter 6). This robustness analysis is presented next together with the resulting restrictions found by using this method. Besides restrictions imposed by the used method, the used model also has limitations which are discussed in the second part of this chapter. In chapter 9 the results are compared to real sandbanks after which the conclusions and recommendations for further research are presented in chapter 10.

8.1 METHOD

The main goal of this research is to determine the influence of the waterdepth on the sandbank characteristics. As explained in section 6.4 it is impossible to execute this research without taking changes of the flow velocity into account. This was done by applying two approaches, a constant flow velocity and a constant water flux, which can be seen as the extremes situations of the development of the flow velocity with increasing waterdepth over time. The actual development of the flow velocity with increasing waterdepth would probably lie in between these two extremes. Additionally the development found for different sandbank characteristics for both approaches would most probably lie in between these extremes.

To be able to compare the influence of the waterdepth on the sandbank characteristics quantitatively for either of the two approaches it is necessary to express the variation in each development of a characteristic against increasing waterdepth. By expressing each variation in percentages it becomes possible to compare the developments of sandbank characteristics to each other. Therefore the following procedure is followed:

For each point the derivative of the line in that point is determined and divided by its value, giving the possible variation of the development within that point in percents i.e. the possible variation of the sandbank characteristic at a certain waterdepth. If this is done for each point within the graph the overall possible variation of the development can be determined by dividing the sum of the percentages by the total amount of points. This way the variation in the value of the sandbank characteristic is estimated due to changes in the waterdepth. The advantage of calculating the percentage derivate of the line in each point instead of determining the average root mean square is that by using this method the gained results are domain independent. Additionally this leads to domain independent conclusions which are of greater value (please note that the conclusions are still bound by other model and method restrictions).

Furthermore the research conducted earlier on sandbank formation assumes the waterdepth and the flow velocity to be constants with a value of 30m and 1.0 ms^{-1} respectively. Therefore it is worthwhile to determine the possible variations in the sandbank characteristics within this point, for which the directional coefficient-method suits very well. The percentage derivate of both lines and the directional coefficient in the points belonging to the waterdepth of H^*=30m for each sandbank characteristic is given below:

Sandbank characteristic	Approach	Directional coefficient at 30m	Percentage at 30m	Average directional coefficient line	Average percentage derivate line
Growth Rate	C.F.V.	$-2.4\ 10^{-4}\ yr^{-1}m^{-1}$	5.7 %	$-5.4\ 10^{-4}\ yr^{-1}m^{-1}$	5.8 %
	C.W.F.	$-6.3\ 10^{-4}\ yr^{-1}m^{-1}$	14.7 %	$-1.4\ 10^{-2}\ yr^{-1}m^{-1}$	15 %
Angle of orientation	C.F.V.	$0.12\ °m^{-1}$	0.6 %	$0.2\ °m^{-1}$	0.5 %
	C.W.F.	$0.34\ °m^{-1}$	1.2 %	$0.3\ °m^{-1}$	0.8 %
Wavelength	C.F.V.	235	3.3 %	232	3.4 %
	C.W.F.	238	3.4 %	214	3.3 %
Migration speed	C.F.V.	$-0.2\ yr^{-1}$	2.4 %	$-0.3\ yr^{-1}$	2.5%
	C.W.F.	$-1.0\ yr^{-1}$	11.3 %	$-9.7\ yr^{-1}$	12.2 %

Table 2: Sensitivity of sandbank characteristics to changes in the Constant Water Flux (C.W.F) or Constant Flow Velocity (C.F.V.)

Although it is difficult to interpret the values given for the directional coefficients, it becomes clear that the average development of the growth rate and migration speed against increasing depth is negative i.e. larger values of the waterdepth give smaller values for the migration speed and growth rate, in accordance with the graphs as presented in chapter 7. But additionally table 2 shows that changes in the growth rate and migration speed are larger for the constant water flux approach than the constant flow velocity approach, which was more difficult to determine from the graphs. The influence of the constant water flux is only smaller for the wavelength, but this difference is marginal.

Furthermore it shows that the angle of orientation is the least sensitive to changes in the waterdepth, regardless of the applied approach. The growth rate is the most sensitive for changes in the waterdepth. The largest difference between the influences of the two approaches appears for the migration speed. Finally it stands out that the values found for the directional coefficient at a waterdepth of 30m is sometimes smaller and sometimes larger than the averaged of the graphs. This indicates that larger changes in the value of the sandbank characteristics are to be expected for certain values of the waterdepth i.e. the average directional coefficient is only an indication of the variation, as locally the variation could be larger or smaller.

Besides taking the possible development of the flow velocity with regard to the waterdepth into account, it was stated that more parameters would most likely not stayed constant over time. Anticipating on this, all input parameters were discussed, section 6.2, and maxima and minima were defined to represent the most extreme developments of these parameters over time. To determine the additional influence of changes in these parameters on the development of the sandbank characteristics against increasing waterdepth, for both approaches the range in the possible development is calculated and expressed in percentages for each sandbank characteristic as follows:

The spreading of a graph with regard to a reference value is given by the mean squared value: the averaged of the sum of all quadratic differences between the points and the reference value. In this case the reference value is the value at a certain waterdepth on the basic line of either $30m^2s^{-1}$ or $1.0ms^{-1}$. The root of the mean square value returns the variation into the same dimensions as the characteristic has, which can be expressed in percentages to be able to compare the sandbank characteristics to each other.

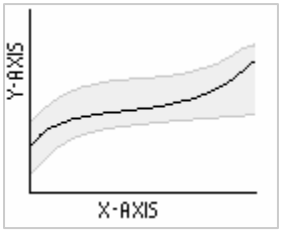

Figure 25: Example of the range of a graph

The range of each sandbank characteristic due to a change in a parameter value is presented below. Do bear in mind that the percentages represent the range of the entire graph and are thus restricted to the domain of the graph: a waterdepth between 10 and 65m.

Parameter	Approach	Growth rate in percentage	Wavelength in percentage	Angle of orientation in percentage	Migration speed in percentage	Average
Flow velocity	C.F.V.	89 %	11 %	5 %	107%	**53 %**
Water flux	C.W.F.	44 %	1 %	3 %	47 %	**24 %**
Drag coefficient	C.F.V.	40 %	145 %	19 %	46 %	**63 %**
	C.W.F.	36 %	138 %	15 %	35 %	**56 %**
Slope parameter	C.F.V.	9 %	18 %	6 %	5 %	**10 %**
	C.W.F.	8 %	18 %	5 %	4 %	**9 %**
Latitude	C.F.V.	1 %	0 %	0 %	1 %	**0.5%**
	C.W.F.	1 %	0 %	0 %	0 %	**0.25%**
	Average	**29 %**	**41 %**	**6 %**	**30 %**	

Table 3: Influences of parameters to the basic lines of the Constant Flow Velocity (C.F.V) and Constant Water Flux (C.W.F) approach per sandbank characteristic expressed in quadratic means and percentage.

The overall conclusions which can be drawn from table 3 are that the wavelength is the most sensitive sandbank characteristic to changes in the parameters; the angle of orientation is the least sensitive. The growth rate and the migration speed are about equally affected by changes in the parameters. Looking at the influence of each parameter specifically, the following dependences stand out:

The wavelength is especially influenced by the drag coefficient (C_D) and the slope parameter (λ^*); the changes in the other parameters hardly influence its development against increasing waterdepth. The angle of orientation is also mostly influenced by the drag coefficient; secondly changes in the slope parameter change its direction compared to the main flow. The migration speed and the growth rate are mainly influenced by changes in the flow velocity, although changes in the water flux and the drag coefficient are of influence too. The applied changes in the latitude (θ) are of no influence on the development of the sandbank characteristics against increasing waterdepth at all.

Changes in the drag coefficient have the largest influence on all sandbank characteristics, regardless of the applied approach. The assumed flow velocity is of importance to the development of the growth rate and the migration speed, and this importance is smaller if the flow velocity is said to be directly dependent on the waterdepth i.e. the constant water flux approach leads to smaller variations in the development compared to that of the constant flow velocity. Changes in the slope parameter have little influence on the development of the sandbank characteristics. The applied changes in the latitude have no effect on the sandbank formation. Supplementary it needs to be remarked that the influence of the flow velocity, the water flux and the latitude can become larger if their value is changed over a larger range, in contrast with the drag coefficient and the slope parameter, which are already varied over their maximum range (section 6.3).

Concluding on the method used to investigate the influence of sea level rise on sandbank morphodynamics it satisfies the first requirements of fundamental research: the results are reproducible and unambiguously interpretable. In contrast, the method used to perform the sensitivity analysis was not very robust as changes in the flow velocity, the water flux, the slope parameter and the drag coefficient do influence the initial formation of sandbanks.

Finally a back coupling needs to be made to the choices made within the performed methodology (section 6.3). First of all it was chosen to include the influence of the latitude into the model of which the possible influence was, looking at the results, overestimated. The applied variation in the values for the flow velocity and the water flux was chosen over a small range to get an indication of their influence. Comparing them to the maximum changes applied in the drag coefficient and slope parameter gives a lame comparison as the amount of variation differs a lot, which could be overcome by enlarging the range of the water flux and flow velocity value. Furthermore it was stated that the tidal frequency (σ^*) was a constant as the dominant tide was the M_2-tide, except for a short period of time. As the flow velocity and the water flux are of great importance for the development of sandbanks, this assumption could very well not be right, especially right after the break-through of the land bridge. Most likely there is flow dominance other than by the M_2 tide, which would result in no sandbank growth at all. In the most positive situation, the development just stood still, instead of partial or total erosion, after which the development resumed.

This would lead to a slower development of the morphology over the same timescale. Besides the tidal frequency the transport formula exponent was considered to be a constant. As there is no physical connection it is hard to determine if changes in its value should be taken into account, once this has become clearer it might be necessary to investigate the influence of this parameter as well.

Although it is permitted to make universal conclusions about the development of the sandbank characteristics against increasing waterdepth for either of the two approaches: a constant water flux or a constant flow velocity over time, the conclusions are limited to the linear regime. This is discussed in more detail in the next section. Furthermore the range is limited to the domain chosen for the waterdepth: if this domain was chosen smaller, or covering a different range of waterdepths, other conclusion could be made. To be able to say anything on the actual influence of parameters on the sandbank characteristics against increasing waterdepth it is necessary to gain more knowledge on the exact development of the southern North Sea.

8.2 MODEL

The model used to examine the influence of sea level rise against increasing waterdepth is a linear model and therefore it was chosen to investigate the influence of different waterdepths on the sandbank characteristics captured within the model. This approach can be seen as static and idealized, as the actual development of sea level rise is time dependent and the change within the fastest growing mode would not adjust perfectly to the circumstances. But a model remains a simplification of reality and within these limitations the following remarks should be made:

Within the linear regime the initial development of sandbanks is seen as instability within the morphodynamical system caused by small perturbations on the sea bottom. In reality it can very well be that (part of) the sandbanks are remains from older sediment which have transformed into sandbanks due to morphological processes. This is in agreement with the results found by Fluit and Hulscher [2002] and Roos and Hulscher [2003]. Geophysical records showing the internal structure of the sandbank will exclude either of these two approaches.

Secondly, assumptions concerning the wind stress at the surface, the wave action, the bottom shear stress and the sediment transport threshold should be considered. Wind stress might be found ignorable at a waterdepth of 30m, but needs to be reconsidered for a depth of 10m. The same holds for the influence of wave action. Changes in the waterdepth lead to changes in the bottom shear stress and it is very well possible that this parameter changes more for changes at shallower depths compared to the same change at deeper depths. Additional the sea bottom does change over time as will the drag coefficient, resulting in other sea bottom stresses and also in other sediment transport rates. Therefore adding a sediment transport threshold might be considered, especially as the results pointed out that the flow velocity is of such importance in the process of sandbank formation.

Finally it is very important to keep in mind that the results found are only an indication of the possible change in sandbank characteristics against increasing waterdepth as it covers only the initial growth. Further research can point out that this might very well not be the case in their further development towards equilibrium. To determine whether or not the results are compatible with reality a comparison with the Dutch Banks, the Flemish Banks and the Zeeland Banks is made in the next chapter.

9 A COMPARISON WITH REALITY

In this chapter a comparison between real sandbanks and the results as gained within this research is made. To be able to make this comparison the fine line between the linear and non-linear regime is crossed, as it is assumed that the results as found in this research also hold for the development of sandbanks towards their equilibrium. Besides the immediate comparison an outlook on the historical and future development of the sandbanks is given, in which the geological development of the North Sea is taken into account. The comparison is based upon the data as presented in the article of Roos et al. [2004] based upon the numerical work of Van der Molen and De Swart [2001].

9.1 PRESENT SITUATION

Analogous to Roos et al. [2004] the comparison takes place between the Dutch Banks, the Flemish Banks and the Zeeland Banks (figure 26). It is not possible to compare real sandbanks on the development of the characteristics migration speed and growth rate as found within this research as: sandbanks in equilibrium do not grow anymore and secondly the estimated migration speed was based upon a steady flow approach, which differs from the flow pattern of elliptical tides resulting in a different migration speed. Therefore analogous to Roos et al. [2004] the comparison shall be made on the wavelength and angle of orientation, accept for the difference that the Zeeland Banks are taken into account here. In their research Roos et al. [2004] conclude that the Zeeland Banks are most probably shoreface connected ridges as their orientation is divergent from other sandbanks in the Northern Hemisphere, clockwise instead of counter clockwise. But to determine if the development of the wavelength against increasing waterdepth is in agreement with reality the Zeeland Banks are included. The other sandbank groups are also compared to each other on the angle of orientation.

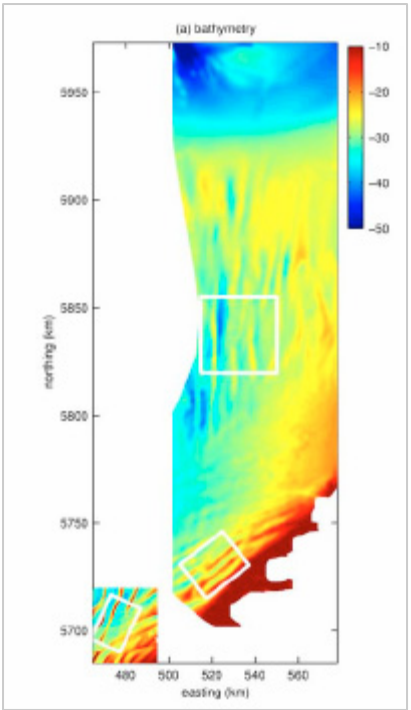

Figure 26: The three sandbank groups:
Upper: Dutch Banks, *Middle:* Zeeland Banks,
Lower: Flemish Banks

Banks	Wavelength	Angle of orientation	Average waterdepth	Flow velocity	Water flux
Dutch Banks	5.7 – 9.8km	25º	28.9m	$1.2ms^{-1}$	$35m^2s^{-1}$
Flemish Banks	4.5km	6º	28.7m	$1.3ms^{-1}$	$37m^2s^{-1}$
Zeeland Banks	~ 5km	--	23m	$1.0ms^{-1}$	$23m^2s^{-1}$

Table 4 Sandbank characteristics, average waterdepth and flow velocity. The flow velocity is estimated from figure X, Appendix E, and the average waterdepth for the Zeeland Banks is estimated from figure 19.

Although these sandbank characteristics can be gained from figures 23 and 24, looking at either the closest line for the constant water flux or that of the constant flow velocity, the values under the basic assumptions (section 6.2) are calculated precisely, resulting in:

Banks	Wavelength	Angle of orientation
Dutch Banks	7.6km	28º
Flemish Banks	8.0km	27º
Zeeland Banks	5.1km	--

Table 5: Model results based upon the average waterdepth and flow velocity.

The model is able to give a rather good agreement with the Dutch Banks and the Zeeland Banks. The results found for the Flemish Banks are not in agreement which can originate from the fact that these banks are often seen as shoreface connected ridges. The abnormality in the angle of orientation is in agreement with the results as found by Roos et al. [2004]. Even though the Zeeland Banks can be seen as shoreface connected ridges as well, the wavelength is in agreement with the model results. The results show that the wavelength increases against increasing waterdepth, as predicted by the model. As the Dutch Banks and the Flemish Banks are located at almost the same waterdepth, no comparison can be made on the development of the angle of orientation against increasing waterdepth.

Although it is easy to blame abnormalities on the possible type distinctions of the sandbanks, there are also some physical processes that are of influence on the appearance of the sandbanks, which are discussed here. First of all the flow velocity should be taken into account as a decrease in velocity leads to a decrease in wavelength. The flow velocity as presented in figure 39 is the sum of all currents present in the southern North Sea, which is different from the M_r tidal current as used within the linear model due to currents enforced by: rivers, other tidal components (like the M_0 and M_4 resulting in tidal asymmetry) or amplification of the M_2 flow velocity near the coast (due to the standing Kelvin wave within the North Sea Basin). Because of such additional currents the flow velocity could be overestimated resulting in overestimation of the wavelength. Secondly the drag coefficient (C_D) should be considered, as a larger roughness of the sea bottom leads to smaller wavelengths. It could very well be that the Flemish Banks are consistent out of coarser material than the Dutch or Zeeland Banks. Finally the slope parameter (λ^*) can play a role as a smaller downhill preference of the sediment transport leads to smaller wavelengths.

As this research revolved around the influence of sea level rise on the development of the sandbanks over time, their appearance is estimated for each of the four time periods which stand out in the formation of the southern North Sea, as given by Van der Molen and De Swart [2001], section 3.2.1.

9.2 DEVELOPMENT OVER THE PAST 9,000 YEARS

To determine the development of the sandbanks over time the average waterdepth during each time period needs to be calculated, which can be done for each sandbank separately by using the Sea Level rise estimation of Beets and Van der Spek, [2000], as given in figure 13. For the Dutch Banks, the line representing the West Netherlands is used, the SLR over the Zeeland Banks is given by the Zeeland Line, and the Flemish Banks are said to be subject to the SLR development within the Belgium Bight. To determine the actual wavelength in the past, both the constant flow velocity approach as well as the constant water flux approach are used, in which the constants are given the value as presented in table 4. Besides the development of the sandbanks based upon changes in the waterdepth, changes in the bathymetry should be taken into account as well as according to Berné et al. [1994] the tidal sandbanks can be separated into two groups based upon the geometry:

1. Sandbanks resting on a flat surface, where bank build-up is only related to a convergent pattern of sand transport. In that case the whole bank consists of Holocene deposits, and
2. Sandbanks whose core consists of eroded fluvial or estuarine sediment or erosive bedrock.

In both cases formation and maintenance of the bank require physical processes at the origin of convergent pattern of sand transport, like the one presented in this research. Nevertheless large deposits during the Holocene need to be taken into account when establishing the development of the wavelength over time, as over time the waterdepth has changed not only due to SLR but also due to Holocene deposits. Beets and Van der Spek [2000] have investigated this deposit pattern near the Dutch and Belgium coasts and discovered that about 60% of the total sediment is deposited before 5,000 years BP, between 5,000 years and 2,900 years BP another 30% was added and the final 10% has been deposited since. In the absence of a more detailed approximation of the division of the Holocene deposits in the other areas of the southern North Sea, this division is used for the estimation of the wavelength during the past 9,000 years.

The total amount of Holocene deposits in the area where the sandbanks are located is determined upon the calculation of Van der Molen and De Swart [2001] (see figure 40 in Appendix E). The total amount of Holocene deposition over the Dutch Banks is said to be 5m, over the Flemish Banks 10m and over the Zeeland Banks 15m. Analogous to section 3.2.1 the wavelength is numerically determined for both approaches during 4 periods, of which the last one contains an outlook to the future development.

PERIOD 1: 9,000 – 8,500 YEARS BP

During this time period 60% of the total Holocene deposits occurred, which would mean that 60% of the entire depth loss due to these deposits should be taken into account, which results in 3, 6 and 9m for the Dutch Banks, Flemish Banks and Zeeland Banks respectively. The average waterdepth over this period is based upon the maximum and minimum value of depth within this period as given in figure 13. The wavelengths are only calculated for waterdepths larger than 10m as this is said to be the lower boundary for sandbank development (section 6.3).

	Waterdepth		Wavelength			
Approach:	Based upon	Rectification	Present		Rectification	
Banks:	present depth	for deposits	C.F.V.	C.W.F.	C.F.V.	C.W.F.
Dutch Banks	12.4m	15.4m	3.3km	5.5km	4.0km	6.0km
Flemish Banks	5.7m	11.7m	x	x	3.2km	5.6km
Zeeland Banks	-5.5m	3.5m	x	x	x	x

Table 6: Wavelength 9,000 – 8.500 years BP for different sandbanks, different waterdepths and both assumptions: Constant Flow Velocity (C.F.V.) and Constant Water Flux (C.W.F.)

If the rectification for Holocene deposits was not taken into account, the Dutch Banks would be the only one present before 8,500 years BP. Their wavelength would lie between half and three-fourth of their present length, which completely depends on the flow velocity. Due to the rectification one can state that the Flemish Banks are most probably of the same age as the Dutch Banks. The estimation of the constant water flux for the wavelength of the Flemish Banks is already larger than the measured value (table 4). It is therefore plausible to conclude that the constant flow velocity approach gives a better representation of their development over time.

PERIOD 2: 8,500 – 7,000 YEARS BP

Again the rectification for Holocene deposits within this time period is 60% of the total deposit, which results into:

	Waterdepth		Wavelength			
Approach:	Based upon	Rectification	Present		Rectification	
Banks:	present depth	for deposits	C.F.V.	C.W.F.	C.F.V.	C.W.F.
Dutch Banks	17.4m	20.4m	4.6km	6.3km	5.4km	6.7km
Flemish Banks	11.2m	17.2m	3.1km	5.5km	4.8km	6.5km
Zeeland Banks	3.5m	12.5m	x	x	2.9km	4.3km

Table 7: Wavelength 8.500 – 7000 years BP for different sandbanks, different waterdepths and both assumptions: Constant Flow Velocity (C.F.V.) and Constant Water Flux (C.W.F.)

Under the assumption of no Holocene deposits the Flemish Banks would just start to develop during this period, with half to two-third of the present wavelength. Of all values given for wavelength of the Flemish Banks, only that under the constant flow velocity and no rectifications for the Holocene deposits is in agreement with the measurements. The wavelengths of both the Dutch Banks and Zeeland Banks can still be in accordance with their present shape.

PERIOD 3: 7,000 – 0 YEARS BP

The rectification for the Holocene deposits equals the total deposits as currently present in the North Sea:

Approach: / Banks:	Waterdepth		Wavelength			
	Based upon present depth	Rectification for deposits	Present		Rectification	
			C.F.V.	C.W.F.	C.F.V.	C.W.F.
Dutch Banks	24.9m	29.9m	6.6km	7.2km	7.9km	7.7km
Flemish Banks	21.5m	31.5m	6.0km	7.1km	8.8km	8.3km
Zeeland Banks	14.5m	29.5m	3.4km	4.5km	6.9km	6.0km

Table 8: Wavelength 7000 – 0 years BP for different sandbanks, different waterdepths and both assumptions: Constant Flow Velocity (C.F.V.) and Constant Water Flux (C.W.F.)

At this point no calculation is in agreement with the measurements of the Flemish Banks. The values found under the Holocene deposits rectification is only in agreement with the dimensions of the Dutch Banks. This could mean that the rectification for the deposited depth over the Zeeland Banks is too large. All values found for the wavelength of the Dutch Banks are in agreement with the measurements.

Summarizing the comparison of the development of the wavelength over time due to sea level rise and rectification for Holocene deposits with the actual dimensions of the sandbanks, the following can be concluded:

The estimation of the wavelength of the Flemish Banks by the linear model is not in agreement with reality. But a thoroughly research to the composition of the Flemish Banks as executed by Berné et al [1994] pointed out that these sandbanks are formed upon Holocene deposits and due to morphodynamic processes moulded into sandbanks. Presently these banks leave their original cores of coarse material after which they would most probably start to behave as 'real tidal sandbanks'. The estimation of the present wavelength of the Zeeland Banks is in agreement with the measurements, but if a rectification for Holocene deposits is taken into account the present wavelength is smaller than the calculation shows. Although an overestimation of the thickness of the Holocene deposits could be pointed out as the problem, their orientation also differs from that of normal sandbanks on the Northern Hemisphere and therefore the possibility that the Zeeland Banks are shoreface connected ridges from origin is still a plausible possibility. The wavelength as estimated with the model shows good agreement with the measured length of the Dutch Banks, even for the Holocene deposits rectification.

But even though the model gives good results one has to take into account that it is only a linear model and therefore gives an indication on the possible wavelength i.e. the preferred development. The fact that there is a similarity supports the fact that the process of sea level rise does influence the development of sandbanks towards their equilibrium. Having concluded this, an outlook to the possible future development of the sandbanks due to continues sea level rise can be given:

PERIOD 4: FUTURE DEVELOPMENT

Presently the sea level rise has a rate of 0.15m per century (section 3.2.1) and as only the directional coefficient of the wavelength under the assumption of a constant flow velocity of 1.0ms^{-1} or a constant water flux of 10m^{2}s^{-1} is known, the following development of the sandbanks can be estimated: an increase in wavelength between the 32m (constant water flux) and 35m (constant flow velocity) a century.

For the Dutch and Flemish Banks, this development shall be faster as an increase in flow velocity leads to an increase in wavelength by as much as 1 to 11%. The opposite holds for the Flemish Banks, as the water flux is smaller than 30m^{2}s^{-1}.

As the results of this research and the procedure to gain them are discussed and a comparison with reality is made, the overall conclusions and recommendations for further research can be made as is done in the final chapter.

10 CONCLUSIONS AND RECOMMENDATIONS

10.1 CONCLUSIONS

In chapter 4 it was demonstrated that the assumption of a constant water level over time to predict the development of sandbanks was not in agreement with reality. To support this hypothesis an example of the Southern Bight of the North Sea was given in which the waterdepth was doubled over the time during which the present sandbanks evolved. By means of a linear model describing the initial development of sandbanks the influence of changes in the waterdepth on the formation of sandbanks was investigated under the assumption of either a constant flow velocity or a constant water flux over time. It appeared that the following changes in the development took place over this time period due to a doubling of the waterdepth:

- A decrease in the growth rate from a value of 4 10^{-3} yr^{-1} (waterdepth = 30m, flow velocity= 1.0 ms^{-1}) to a rate between 1.3 10^{-3} and 2 10^{-4} yr^{-1}
- A decrease in the migration speed from a value of 9.1 10^{-3} km per year (waterdepth = 30m, flow velocity= 1.0 ms^{-1}) to a rate between 5.4 10^{-3} and 7 10^{-4} km per year
- An increase of the angle of orientation from a value of 29º (waterdepth = 30m, flow velocity= 1.0 ms^{-1}) to a angle between 34º and 39º
- An increase in the wavelength from a value of 7 km (waterdepth = 30m, flow velocity= 1.0 ms^{-1}) to a length between 14 and 15 km

It can therefore be concluded that the influence of sea level rise on sandbank morphodynamics should be taken into account as it changes its characteristics dramatically.

Besides changes in the waterdepth, the process of sea level rise also includes changes in other morphodynamical processes. In this research the influence of changes in the flow velocity (U^*), the water flux (H^*U^*), the drag coefficient (C_D), the slope parameter (λ^*) and the latitude (θ) were taken into consideration. It shows that for the applied variation in the values:

- Changes in the flow velocity and water flux lead to a change in the growth rate and migration speed of 67 and 77% respectively.
- Changes in the drag coefficient lead to changes in all four sandbank characteristics by as much as 56 to 63%.
- Changes in the slope parameter affect mostly the wavelength by as much as 18%.
- Changes in the latitude do not affect the sandbank characteristics.

Ergo the process of sea level rise should be seen broader than just a change in the waterdepth over time.

Although this research has given insight in the influence sea level rise on morphodynamics of sandbanks, it is just a first exploring investigation as it handles the preferred sandbank characteristics and the basic processes of sea level rise. Therefore the following recommendations can be made.

10.2 Recommendations

In the framework of this project the process of sea level rise was implemented within the linear model describing the initial formation of sandbanks by changing the waterdepth. Additionally the processes that depend on changes in the waterdepth, like the flow velocity, were considered. As explained in chapter 8, due to the results found the influence of changes in the value of other parameters should be considered as well. Furthermore it was said that for each change in waterdepth the additional fastest growing mode would change to its optimum. It is not said that this would happen in reality as more processes influence this shift. Thirdly the process of sea level rise involves more than just a change in waterdepth also the Earth's crust changes due to relaxation and the oceans volume expand due to heat storage. Movements in the crust will affect sea-bottom features and water density properties might affect the flow pattern. In which way these factors affect the formation of sandbanks or should be taken into consideration when adding waterdepth changes to the model, needs to be established through further research.

But before such detailed research is performed it is more important to investigate whether or not the found dependence between waterdepth changes and sandbank morphodynamics holds within the non-linear regime i.e. if the sandbanks are also affected by changes in the waterdepth in their development towards equilibrium. Within such a research attention should be paid to the additional influences of changes in other parameters besides the ones mentioned in the linear regime. Because within the non-linear regime more processes are responsible for the development of the sandbanks and these processes might be affected by sea level changes as well.

Apart from the research which can be performed through modelling, it is important to investigate the composition of sandbanks. This will enhance the insight in their formation as based upon soil samples, the growth rate over time as well as the migration speed can be determined. Information on their composition also answers the question of sandbanks can be seen as instabilities within the morphological system or are ancient features which have been subjacent to morphological processes and changed into sandbanks, as every kind of instability of the bed would evolve into a sandbank according to Roos and Hulscher [2003]. This knowledge would explain possible differences in the outcome of the models and the actual appearance of the sandbanks.

Now that has become clear that assuming a constant waterdepth has great consequences for the initial formation of sandbanks, it is imaginable that the interest in the influence of other processes as presented in section 2.3.6 is strengthened. Perhaps did this research not only arouse the interest in the field of sandbanks but also in that of other sea bottom features for which changes in the waterdepth may be of influence. At least I hope to have given more insight into the dependence of the processes of sandbank morphodynamics to changes in the waterdepth and I hope further research that is conducted will lead to full understanding of sandbank formation, as that would lead to expertise applicable to many seabed related problems like the potential exposure of pipelines and the grounding of ships.

11 REFERENCES

[Antonov, 2002]
John i. Antanov, Steric sea level variations during 1957 – 1994: Importance of salinity, Journal of geophysical Research Vol. 107, 8013 – 8027, 2002.

[Beets, Van der Spek, 2000]
Dirk, J, Beets & Adam J.F. van der Spek, The Holocene evolution of the barrier and the back-barrier basins of Belgium and the Netherlands as a function of late Weichselian morphology, relative sea-level rise and sediment supply, Geologie en Mijnbouw, Vol. 79, 3 – 16, 2000.

[Belderson et al, 1986]
R.H. Belderson, R.D. Pingree, D.K. Griffiths, Low sea-level tidal origin of Celtic Sea sand banks – evidence from numerical modelling of M2 tidal streams, Marine Geology Vol. 73, 99 – 108, 1986.

[Berné et al, 1994]
S. Berné, A. Trentesaux, A.Stolk, T. Missiaen, M. de Batist, Marine geology, international journal of marine geology, chemistry and geophysics, Marine Geology 121m 57 – 72, 1994.

[Brown et al, 2000]
Evelyn Brown, Angela Colling, Dave Park, John Phillips, Dave Rothery, John Wright, Waves, tides and shallow-water processes, second edition, Hst 2, 2000.

[Cameron et al, 1993]
D. Cameron, D van Doorn, C. Laban, H.J. Streif, Geology of the Southern North Sea Basin, reprint from Coastlines of the Southern North Sea, 19-23, 1993.
[Caston, 1981]
G.F. Caston, Potential gain and loss of sand banks in the Southern Bight of the North Sea, Marine Geology Vol. 41,239 - 250, 1981.
[De Mulder et al, 2003]
Ed F.J. Mulder, Mark C. Geluk, Ipo Ritsema, Wim E. Westerhoff en Theo E. Wong, De ondergrond van Nederland, Geologie van Nederland (deel 7), deel 2, 2003.
[De Vriend, 1990]
H.J de Vriend, Morphological processes in hallow Tidal Seas, Residual currents and long term transport, R.T.Cheng editor, Verslag , Coastal and Estuarine Studies, 38, 276 - 301, 1990.
[Douglas, 1991]
Bruce C. Douglas, Global Sea Level Change: Determination and interpretation, Rev. Geophysics. Vol. 33,
[http://www.agu.org/revgeophys/dougla01/dougla01.html]
[Douglas, 1997]
Bruce C. Douglas, Global sea rise: a redetermination, Surveys in Geographic Vol. 18, 279 - 292, 1997.
[Douglas & Peltier, 2002]
Bruce C. Douglas, W. Richard Peltier, The puzzle of Global Sea - Level Rise, Physics Today Vol. 55 (3), 35 - 45, 2002.
[Dyer & Huntley, 1999]
Keith R. Dyer and David A. Huntley, The origin, classification and modelling of sand banks and ridges, Continental Shelf Research, Vol. 19, 1285 - 1330, 1999.
[Fluit & Hulscher, 2002]
Caroline C.J.M. Fluit and Suzanne J.M.H. Hulscher, Morphological response to a North Sea bed depression induced by gas mining, Journal of Geophysical Research Vol. 107, 10.1029, 2002.
[Hallam, 2001]
A. Hallam, a review of the broad pattern of Jurassic sea-level changes and their possible causes in the light of current knowledge, Palaeography, Palaeoclimatology, Palaeoecology 167, 23 - 37, 2001.
[Harris, 1988]
P.T. Harris, Large scale bedforms as indicators of mutually evasive sand transport and the sequential infilling of wide-mouthed estuaries. Sedimentary Geology Vol. 57, 273 - 298, 1988.
[Hulscher et al, 1993]
Suzanne J.M.H. Hulsher, Huib E. de Swart and Huib J. de Vriend, The generation of offshore tidal sand banks and sand waves, Continental Shelf Research Vol. 13 (11), 1183 - 1204, 1993.

[Hulscher, 1996]
Suzanne J. M. H. Hulscher, tidal-induced large-scale regular bed form patterns in a three-dimensional shallow water model, Journal of Geophysical Research Vol. 101 No C9, 20,727 – 20,744, 1996.

[Huthnance, 1982]
John M. Huthnance On one mechanism forming linear sand banks, Estuarine, Coastal and Shelf Science, Vol. 14, 79 – 99, 1982.

[Idier & Astruc, 2003]
Deborah Idier and Dominique Astruc, Analytical and numerical modelling of sand banks dynamics, Journal of Geophysical Research Vol. 108 (C3), 10.1029, 2003.

[Jansen et al, 1983]
E. Jansen, H.P. Serjup, T.Ejaeran, M. Hald, H. Holtedahl en O.Skarbo, Late Weichselian paleoceanography of the southeastern Norwegian Sea, Norsk. Geolog. Tidsskr. 63, 117 – 146, 1983.

[Janssen et al, 1990]
P.H.M. Janssen, W.Slob en J.Rotmans, Gevoeligheidsanalyse en Onzekerheidsanalyse, een inventarisatie van Ideeën, Methoden en Technieken, Rijks instituut voor volksgezondheid en milieuhygiëne Bilthoven, 1990.

[Jelgersma, 1979]
Saskia Jelgersma, Sea-level changes in the North Sea basin, The Quaternary History of the North Sea, Univ. Ups. Annum Quingentesimum Celebrantis 2, Uppsala. 233 - -248, 1979.

[Komarova & Newell, 2000]
Natalia L. Kamarova and Alan C. Newell, Nonlinear dynamics of sand banks and sand waves, Journal of Fluid Mechanics Vol. 415, 285 – 321, 2000.

[Komarova & Hulscher, 2000]
N.L. Kamarova and S.J.M.H. Hulscher, Linear instability mechanisms for sand wave formation, Journal of Fluid mechanics, Vol. 413, 219 – 246, 2000.

[Labau, 1995]
C. Labau, The pleistocene glaciations in the Dutch sector of the North Sea PhD thesis, University of Amsterdam, 1995.

[Lambeck, 1989]
K. Lambeck, Glacial rebound, sea level change and mantle viscosity, Q. J. Roy Astron Soc 31, 1 – 30, 1989.

[Levitus et al, 2001]
Sydney Levitus, John I. Antanov, Julian Wang, Thomas L. Delworth. Keith W. Dixon, Anthony J Broccoli, Anthropogenic Warming of Earth's Climate System, Science Vol. 292 Issue 5515, 267 – 270, 2001.

[Miller, Douglas, 2004]
Laury Miller, Bruce C. Douglas, Mass and volume contributions to twentieth-century global sea level rise, Nature Vol. 428, 406 – 409, 2004.

[Munk, 2003]
Walter Munk, Ocean Freshening, Sea Level Rising, Science Vol. 300, 2041 – 2043, 2003.

[Off, 1963]
T. Off, Rythmic linear sand bodies caused by tidal currents, Bulletin of the American Association of Petroleum Geology Vol. 47, 324 – 341, 1963.

[Roos et al, 2004]
Pieter C. Roos, Suzanne J.M.H. Hulscher and Michiel A.F. Knaapen, The cross-sectional shape of tidal sand banks: Modelling and observations. Journal of Geophysical research, Vol. 109, 10.1029, 2004.

[Roos & Hulscher, 2003]
Pieter C. Roos and Suzanne J.M.H. Hulscher, Large-scale seabed dynamics in offshore morphology: Modelling human intervention, Reviews of Geophysics, Vol. 41/2, 10.10, 10.1029, 2003.

[Swift, 1975]
D.J.P. Swift, Tidal sand ridges and shoal-retried massifs, Marine Geology Vol. 18, 105 – 133, 1975.

[Terwindt, 1971]
J.H.J. Terwindt, Sand waves in the Southern Bight of the North Sea, Marine Geology Vol. 10, 51 – 67, 1971.

[Van Malde, 1996]
J van Malde, Historical extraordinary water movements in the North Sea area, The hydrographic journal (86), 17 – 24, 1996.

[Van der Molen & De Swart, 2001]
J. van der Molen, H.E. de Swart, Holocene tidal conditions and tide-induced sand transport in the southern North Sea, Journal of geophysical research Vol. 106 (C5), 9339 – 9362, 2001.

[Van Dijck, 1999]
Bastian van Dijck, Holocene coastal evolution of the south-eastern part of the north Sea, Institute for marine and atmospheric research Utrecht, 1999.

[Van Rijn, 1993]
L.C. van Rijn, Handbook of sediment transport by currents and waves, Aqua, Amsterdam, Netherlands, 1993.

[Vithana, 2002]
H.P. Viduragimo Vithana, Predicting offshore large-scale morphology for sustainable use if marine seabed in the North Sea – a research proposal, 2002.

[www.caperomain.fws.gov]
http://www.caperomain.fws.gov, visited, 05/23/05

[www.imedea.uib.es]
http://www.imedea.uib.es/Oceanography/html/research/Projects/WEB_ecbi/fotos/Ibiza_maintenance_180602/ (visited 02/28/05)

[www.noordzee.org]
http://www.noordzee.org, visited 06/28/05

[www.nodc.noaa.gov]
http://www.nodc.noaa.gov/woce_V2/disk 09/psmsl.hel, visited on 02/10/05

[www.deepcovekayak.com]
http://www.deepcovekayak.com/location/destinations/descrip/river.html, visited 04/18/05

APPENDIX A: THE GROWTH RATE

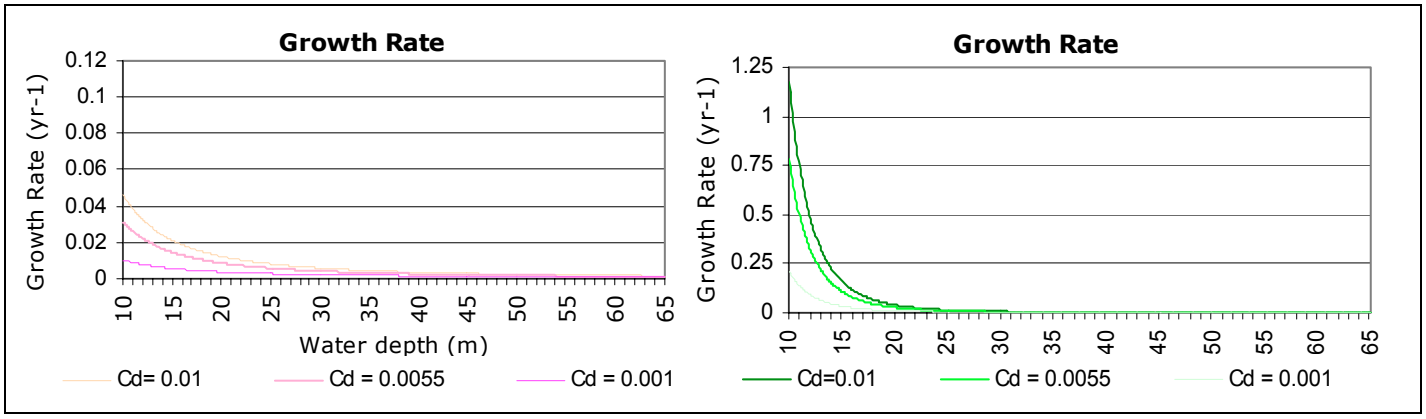

Figure 27: Growth Rate against increasing waterdepth for different values of the drag coefficient; *Left*: Constant Flow Velocity, *Right*: Constant Water Flux.

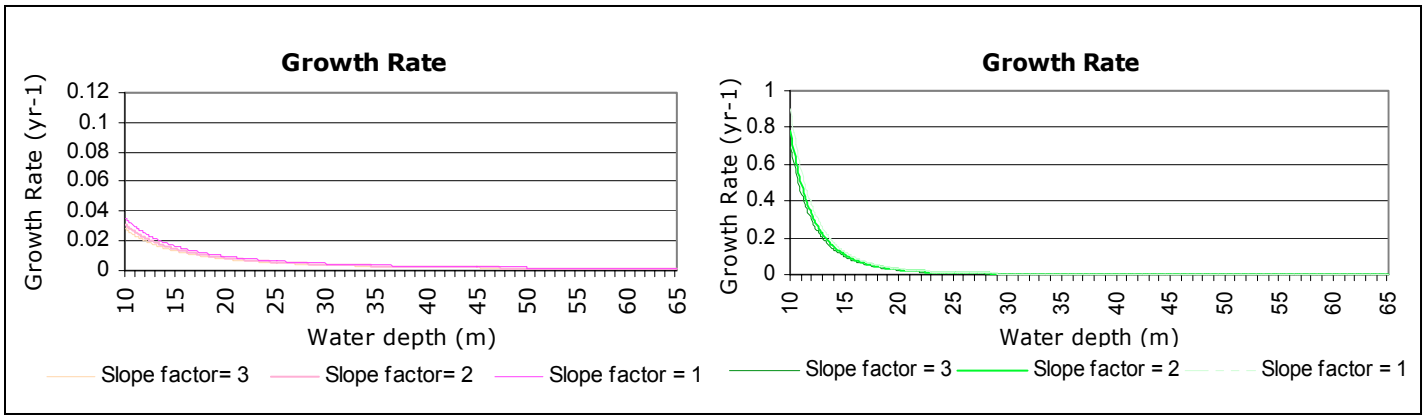

Figure 28: Growth Rate against increasing waterdepth for different values of the slope factor; *Left*: Constant Flow Velocity; *Right*: Constant Water Flux.

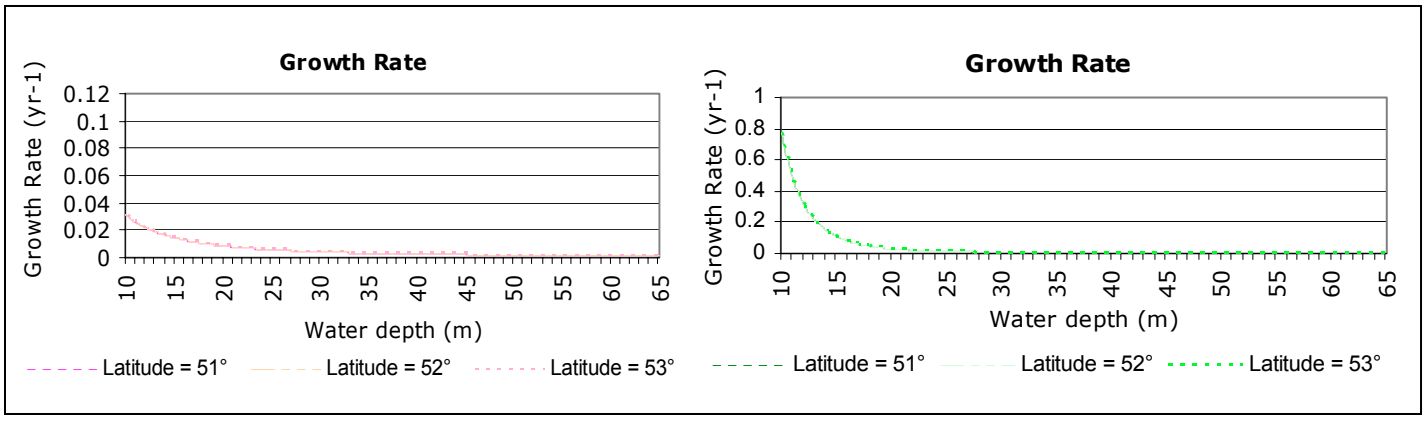

Figure 29: Growth Rate against increasing waterdepth for different values of the latitude; *Left*: Constant Flow Velocity; *Right*: Constant Water Flux.

APPENDIX B: ANGLE OF ORIENTATION

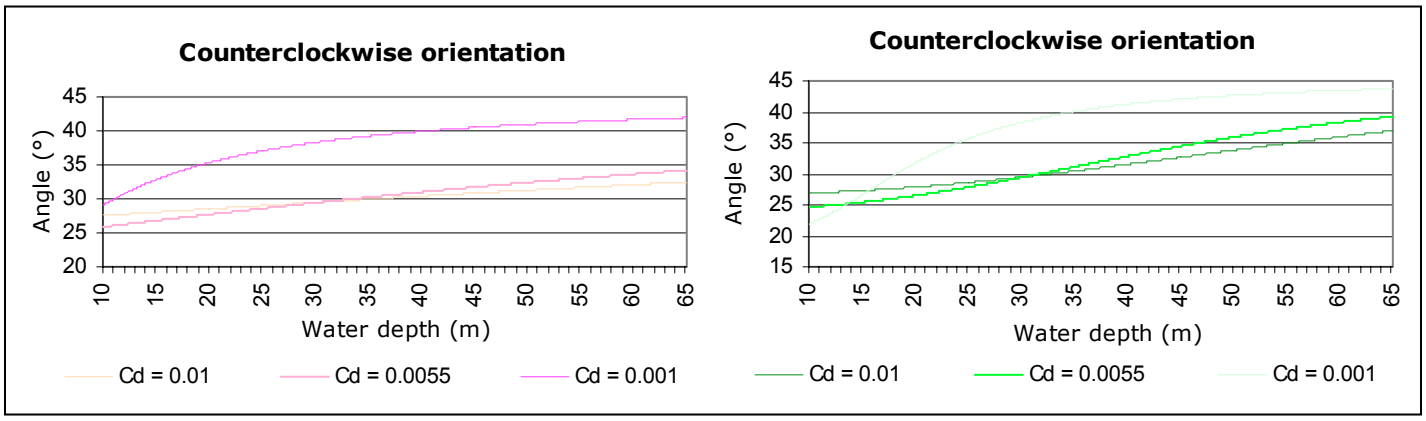

Figure 30: Counter clockwise angle of orientation against increasing waterdepth for the drag coefficient; *Left*: Constant Flow Velocity; *Right*: Constant Water Flux

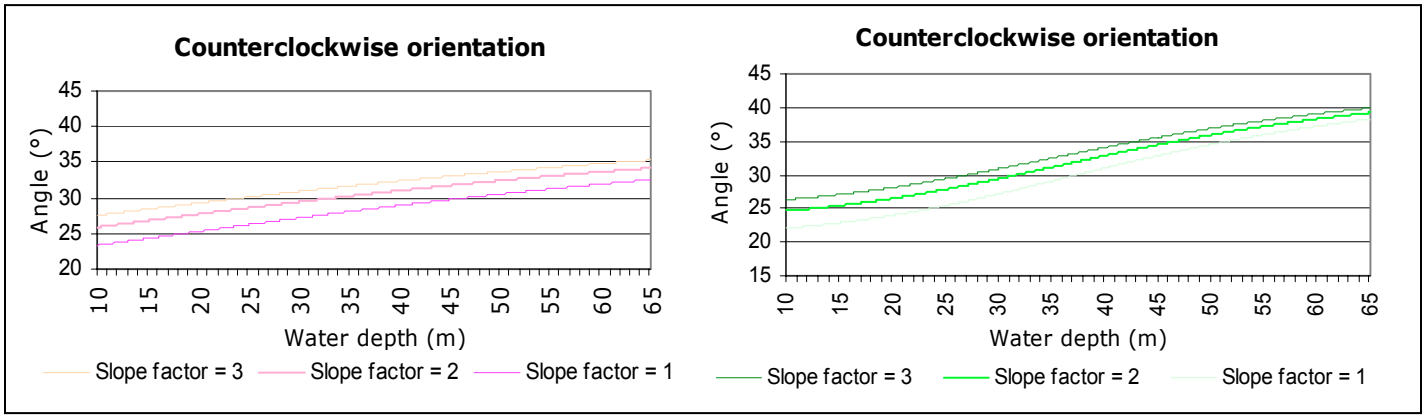

Figure 31: Counter clockwise angle of orientation against increasing waterdepth for the slope factor; *Left*: Constant Flow Velocity; *Right*: Constant Water Flux

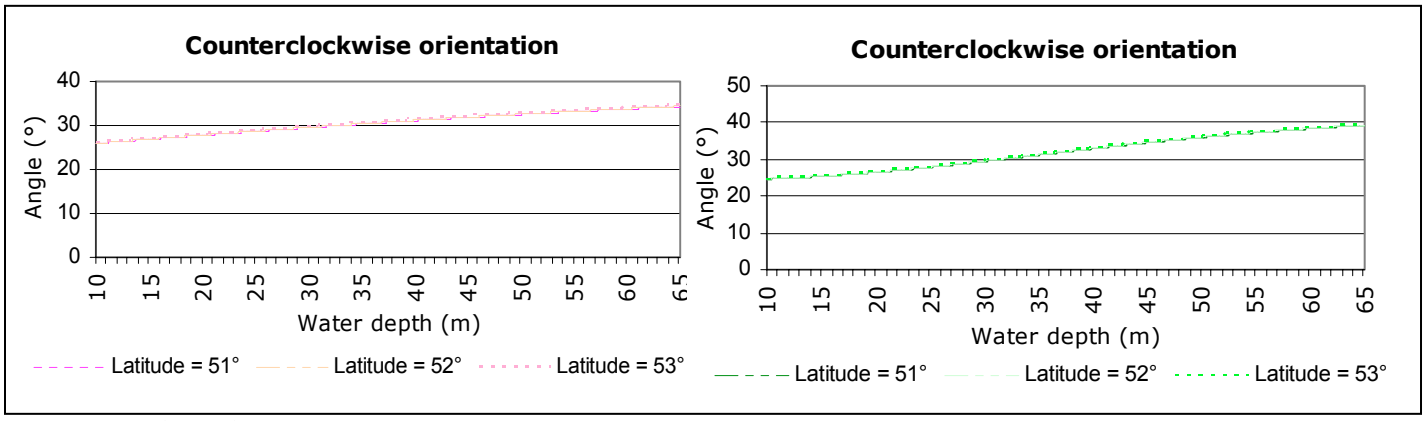

Figure 32: Counter clockwise angle of orientation against increasing waterdepth for the latitude; *Left*: Constant Flow Velocity; *Right*: Constant Water Flux

APPENDIX C: THE WAVELENGTH

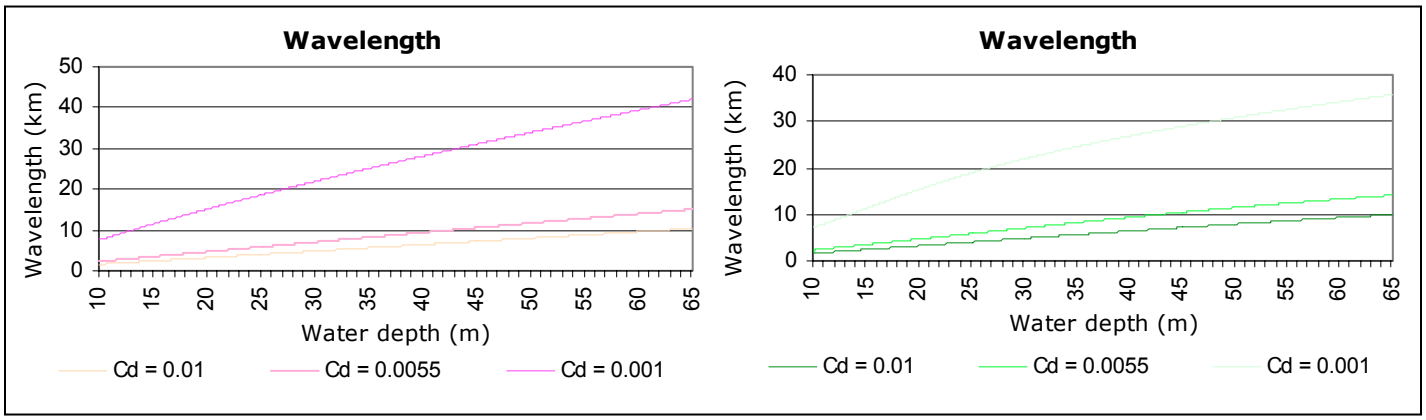

Figure 33: Wavelength against increasing waterdepth for the drag coefficient;
Left: Constant Flow Velocity; *Right*: Constant Water Flux

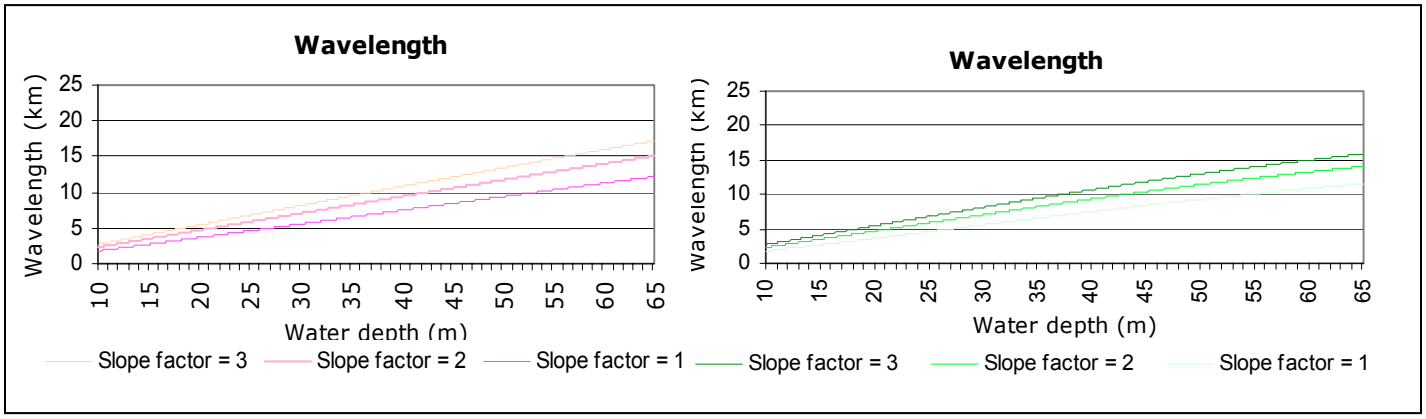

Figure 34: Wavelength against increasing waterdepth for the slope parameter;
Left: Constant Flow Velocity; *Right*: Constant Water Flux

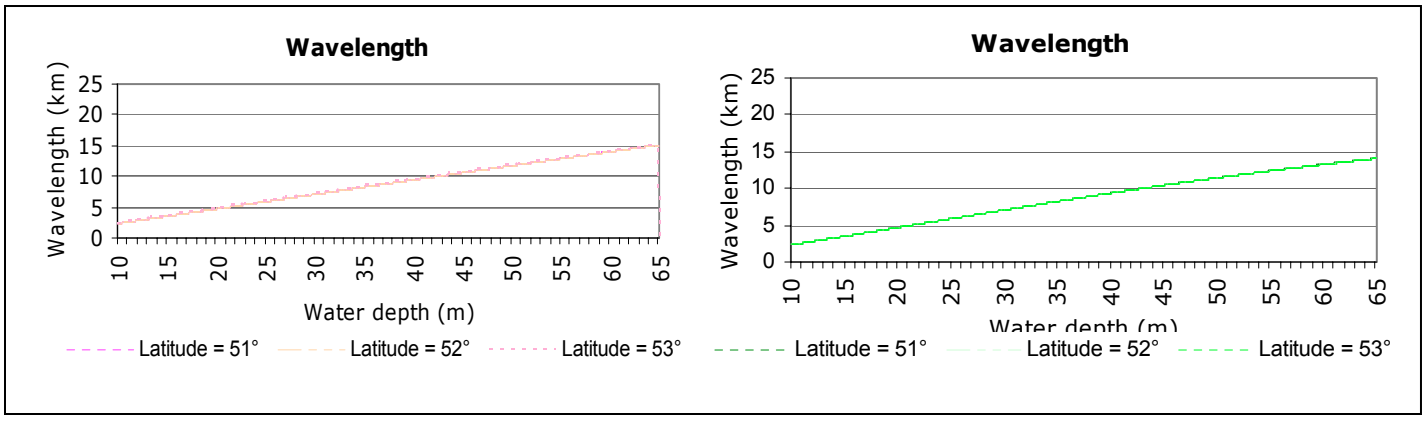

Figure 35: Wavelength against increasing waterdepth for the latitude;
Left: Constant Flow Velocity; *Right*: Constant Water Flux

APPENDIX D: THE MIGRATION SPEED

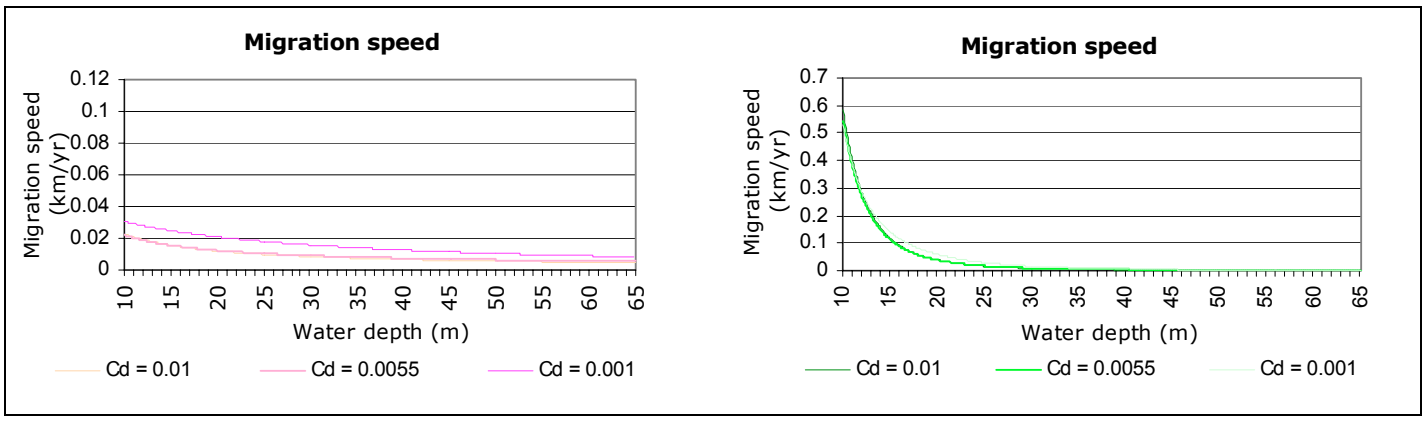

Figure 36: Migration speed against increasing waterdepth for the drag coefficient;
Left: Constant Flow Velocity; *Right*: Constant Water Flux

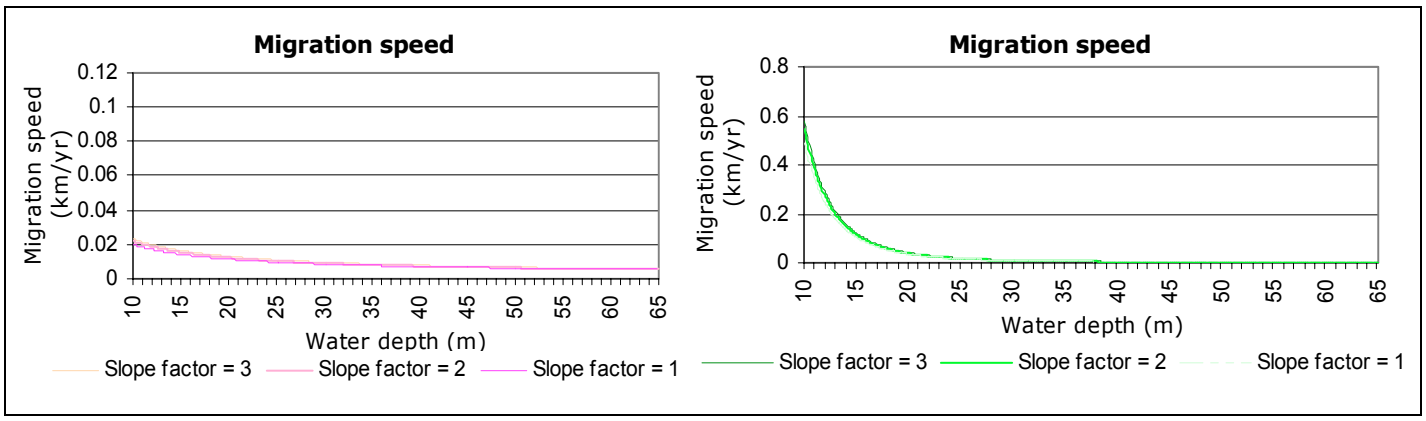

Figure 37: Migration speed against increasing waterdepth for the slope factor;
Left: Constant Flow Velocity; *Right*: constant water flux

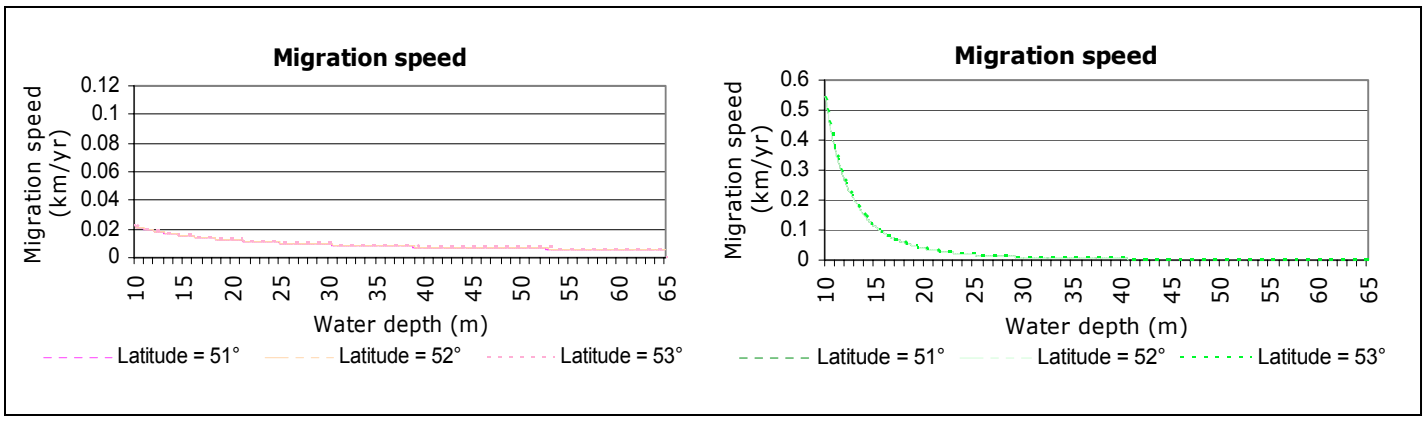

Figure 38: Migration speed against increasing waterdepth for the latitude;
Left: Constant Flow Velocity; *Right*: Constant Water Flux

APPENDIX E: COMPARISON WITH REALITY

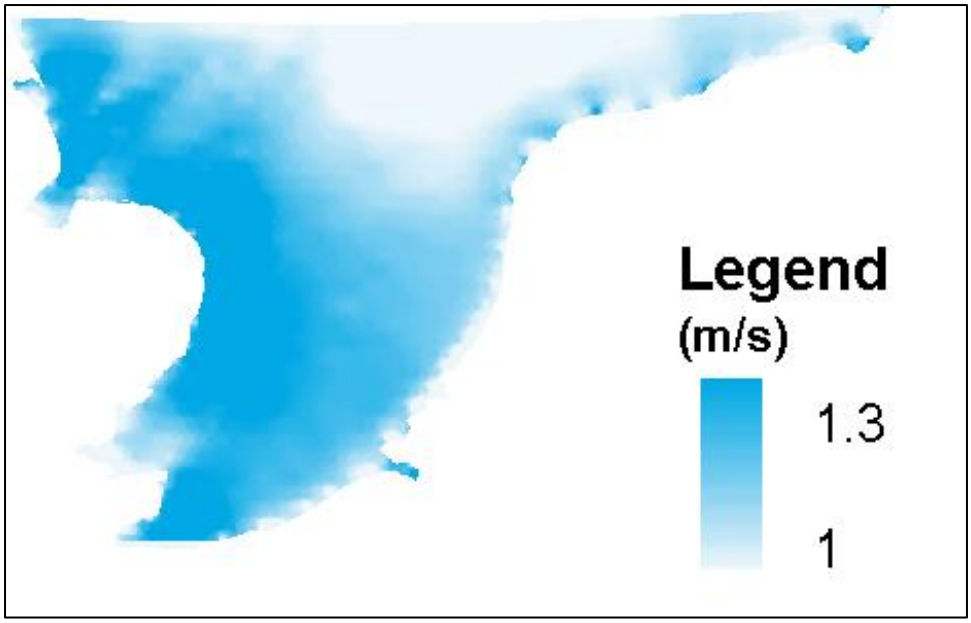

Figure 39: The average flow velocity in the North Sea.

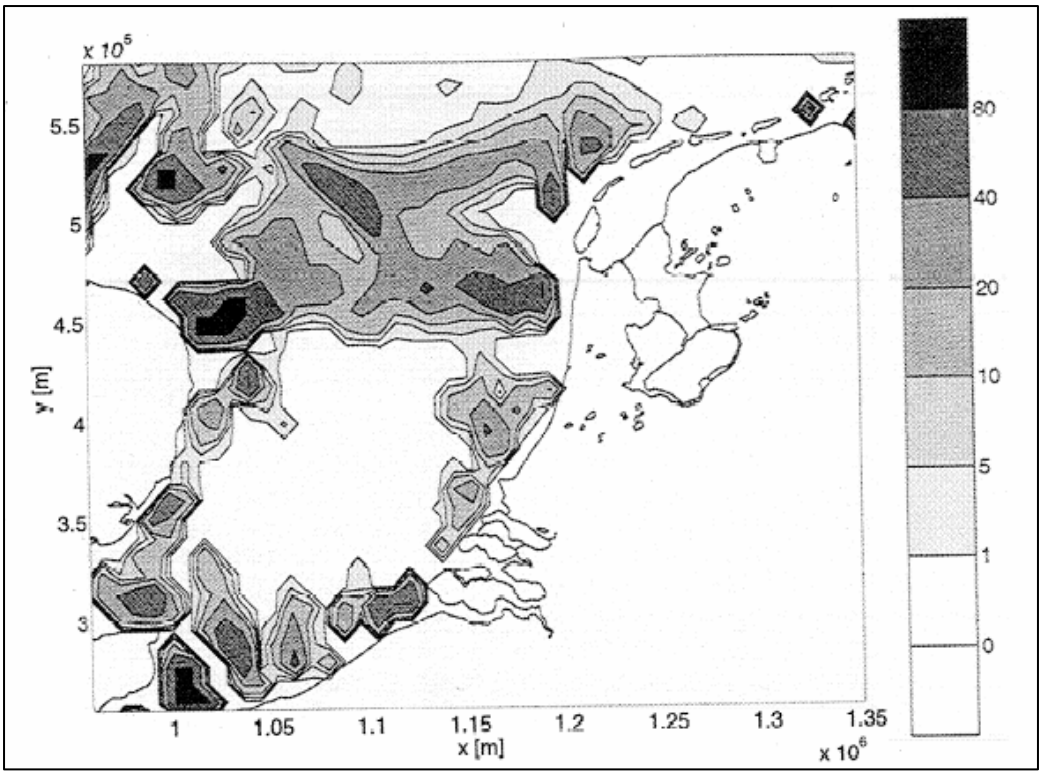

Figure 40: Holocene sediment deposits in the Southern North Sea [Van der Molen & de Swart, 2001]